Exxon Valdez Oil Spill
Restoration Project Final Report

Geomorphic Position, Weathering, and Possible Biotic Impacts of Oil Mousse Persisting on a High Energy Coastline Distant from the *Exxon Valdez* Spill

Restoration Project 94266-1
Final Report

Gail V. Irvine
USGS-Biological Resources Division
Alaska Science Center
1011 East Tudor Road
Anchorage, AK 99503

Daniel H. Mann
Alaska Quaternary Center
and
Institute of Arctic Biology
907 Yukon Drive
University of Alaska
Fairbanks, AK 99775

Jeffrey W. Short
National Marine Fisheries Service, NOAA
Alaska Fisheries Science Center
Auke Bay Laboratory
11305 Glacier Highway
Juneau, AK 99801

April 1997

Exxon Valdez Oil Spill
Restoration Project Final Report

Geomorphic Position, Weathering, and Possible Biotic Impacts of Oil Mousse Persisting on a High Energy Coastline Distant from the *Exxon Valdez* Spill

Restoration Project 94266-1
Final Report

Gail V. Irvine
USGS-Biological Resources Division
Alaska Science Center
1011 East Tudor Road
Anchorage, AK 99503

Daniel H. Mann
Alaska Quarternary Center
and
Institute of Arctic Biology
907 Yukon Drive
University of Alaska
Fairbanks, AK 99775

Jeffrey W. Short
National Marine Fisheries Service, NOAA
Alaska Fisheries Science Center
Auke Bay Laboratory
11305 Glacier Highway
Juneau, AK 99801

April 1997

Stranded Oil Persistence along National Park Coasts

Main Body Title:
Geomorphic Position, Weathering, and Possible Biotic Impacts of Oil Mousse Persisting on a High Energy Coastline Distant from the Exxon Valdez Spill

Restoration Project 94266-1
Final Report

Study History: Restoration Project 94266 was initiated as part of the Oiled Mussel Project in 1992 (R103B), which later became 93090. An interim status report was submitted in 1993 by C. Schoch, under the title 1992 Stranded Oil Persistence Study on Kenai Fjords National Park and Katmai National Park and Preserve. In 1994, it was moved under project 94266: Shoreline Assessment and Oil Removal, though its intent and objectives were quite different from that umbrella project. A draft interim status report (=annual report) was submitted in April 1995 by Mann, D., Irvine, G., and Cusick, J., entitled Fate and Persistence of Oil Stranded on Gulf of Alaska Shorelines during the 1989 *Exxon Valdez* Oil Spill. The main body of the present report has been published as: Multi-year persistence of oil mousse on high energy beaches distant from the *Exxon Valdez* spill origin, 1999, by Irvine, G.V., D.H. Mann, and J.W. Short, in Marine Pollution Bulletin 38(7): 572-584.

Abstract: We describe the geomorphic settings and polynuclear aromatic hydrocarbon (PAH) alteration through time of *Exxon Valdez* oil stranded as mousse on the coastline of Katmai National Park and Preserve, 480-640 km from the site of the spill. At these distal sites, wave energy is higher and coastal geomorphology is fundamentally different from Prince William Sound. Oil has persisted on beaches with an armor of large lag boulders where it has weathered little since arriving five years ago, in 1989. Comparisons of mousse sampled in 1989, 1992, and 1994 indicate only negligible changes in polynuclear aromatic hydrocarbon (PAH) abundances for 22 of 25 samples collected. Five-year old oil strongly resembles 11-day old *Exxon Valdez* crude sampled after the spill. The slowness of chemical weathering of the oil is related to: 1) oil arriving in the form of mousse, and 2) the stranding of oil high in the intertidal zone under boulders where it is protected most from wave action, wind, and sunlight. Although, the biotic effects of oil persisting on the Katmai coast probably are slight, persistent oil still has the potential to affect biota if it is released through disturbance of the armoring substrate, e.g., through unusually high energy wave events.

Key Words: Alaska, *Exxon Valdez*, geomorphology, national parks, oil, oil mousse, persistence, polynuclear aromatic hydrocarbons (PAH), weathering

Project Data: The data collected by this project include: 1) description of oiling at selected sites along Kenai Fjords and Katmai National Parks; 2) quantitative percent cover estimates of persistent oiling within permanently marked quadrats; 3) chemical analyses via gas-chromatography, mass-spectroscopy of oil samples collected by this project in 1992 and 1994, as well as some historical samples collected in 1989. Descriptions of oiling and the percent

coverages are expressed fully in the text and tables of the report (data are descriptive and tabular); Gail Irvine is the custodian of these data (U.S.G.S.-B.R.D., Alaska Science Center, 1011 East Tudor Road, Anchorage, Alaska 99503, phone 907/786-3653, fax 907/786-3636, E-mail gail_irvine@usgs.gov). The hydrocarbon data are held as part of a larger database, The Exxon Valdez Oil Spill of 1989: State-Federal Trustee Council Hydrocarbon Database (EVTHD), 1989-1995. This database is housed at the Auke Bay Labs with Bonita Nelson as custodian (11305 Glacier Highway, Juneau, Alaska 99801-8626, phone 907/789-6071, fax 907/789-6094, E-mail bnelson@abl.afsc.noaa.gov). Data are available on diskette in multiple formats.

Citation: Irvine, G.V., D. H. Mann, and J. W. Short. 1996. Geomorphic position, weathering, and possible biotic impacts of oil mousse persisting on a high energy coastline distant from the *Exxon Valdez* spill. *Exxon Valdez* Oil Spill Restoration Project Final Report (Restoration Project 94266-1), U.S. Geological Survey, Anchorage, Alaska.

TABLE OF CONTENTS

LIST OF TABLES

LIST OF FIGURES

LIST OF APPENDICES

Geomorphic Position, Weathering, and Possible Biotic Impacts of Oil Mousse Persisting on a High Energy Coastline Distant from the *Exxon Valdez* Spill

EXECUTIVE SUMMARY

Previous studies of shore-zone impacts by oil spilled from the *Exxon Valdez* focus on sites proximal to the spill in Prince William Sound. Characteristically, these sites experience relatively low wave energy and were contaminated by fluid crude oil.

We describe the geomorphic settings and polynuclear aromatic hydrocarbon (PAH) alteration through time of *Exxon Valdez* oil stranded as mousse on the coastline of Katmai National Park and Preserve, 480-640 km from the site of the spill. At these distal sites, wave energy is typically higher, and coastal geomorphology is fundamentally different than in Prince William Sound. Along the Katmai coast, recent sea level has been more stable because the 1964 earthquake had only minor effects there, and non-bedrock shorelines are more widespread.

Initial oiling occurred sporadically along the Katmai coast. Much of the initially deposited oil was either buried by sediments or removed by wave action, except on beaches with an armor of large lag boulders.

However, where it has persisted, oil has weathered little in the five years since 1989. Comparisons of mousse sampled in April 1989, autumn 1989, July/August 1992, and August 1994 indicate only small changes in polynuclear aromatic hydrocarbon (PAH) abundances for 22 of 25 samples collected.

The slowness of weathering of the oil is related to several factors. Oil on the Katmai coast initially arrived in a more weathered state than it did in Prince William Sound. In mousse, the surface of oil available for weathering is less per volume than for more fluid

oil. Consequently, mousse may be more recalcitrant to weathering than fresher, more mobile oil. The oil along the Katmai coast typically persists at sites high in the intertidal zone under boulders where it is protected from most wave action, wind, and sunlight.

The biotic effects of oil persisting on the Katmai coast probably are slight because the oil stranding was initially patchy and ultimately persisted only high in the intertidal of boulder beaches where marine plants and invertebrates are characteristically sparse. However, persistent oil still has the potential to affect biota if it is released through disturbance of the armoring substrate, e.g., through unusually high-energy wave events.

INTRODUCTION

As crude oil from the wreck of the *Exxon Valdez* drifted southwest out of Prince William Sound on the Alaska Coastal Current, it was transformed by evaporation and mixing with seawater into mousse. Rafts of oil mousse were stranded sporadically along the Gulf of Alaska coastlines of the Kenai Peninsula and the Alaska Peninsula (Figure 1). Although only 2-4% of the total *Exxon Valdez* spill came ashore on the coastlines of the Shelikof Strait (Wolfe et al., 1994), this contamination compromised the aesthetics and wilderness values of Katmai National Park and Preserve, one of the most pristine wilderness-coast parklands in the world. The critical questions became how long the oil would persist and what geomorphic settings were correlated with its persistence. Additional concerns centered on the possible biological consequences of persistent oil contamination.

Exxon and several different government agencies monitored the changing amounts of stranded oil on Gulf of Alaska shorelines receiving cleanup. However, no heavily impacted, Gulf of Alaska shorelines were set aside as controls to study the fate and persistence of stranded mousse under natural weathering conditions. Because much of the oil stranded on Gulf of Alaska shorelines was oil mousse rather than freshly spilled crude oil, results of NOAA studies on crude oil weathering and persistence on shorelines inside Prince William Sound (Michel and Hayes, 1993a, b; 1994; 1996) may not be applicable to areas in the Gulf of Alaska. The Katmai coast differs markedly in typical wave energy and coastal geomorphology from much of Prince William Sound.

Though oil contamination was usually much less intensive on Gulf of Alaska shorelines distal to the spill, it was spatially extensive. More than 750 linear kilometers of the Gulf of Alaska coastline outside of Prince William Sound were sporadically contaminated (Figure 1). Distance from the spill point also translates into time elapsed, and increasing exposure of the oil to air and water processes (evaporation, dissolution, etc.) is expected to translate into increased weathering of the oil. However, when mousse (a viscous water-in-oil emulsion containing up to 70% water; Payne et al., 1983) is formed, the surface area of oil exposed to weathering processes is lessened and consequently, so is the rate of weathering. Of concern is whether formation and long-distance transport of mousse results in delivery of a still-toxic form of oil to affected areas.

OBJECTIVES

The objectives of our study were to determine: 1) how long oil contamination persists in worst-case situations, 2) how the PAH composition changed during weathering, and 3) what relationship exists between coastal geomorphology and where stranded oil persists.

STUDY AREA

Bedrock Geology and Tectonics

The southeastern Alaskan Peninsula (Figure 2) is formed of Mesozoic aged sedimentary rocks intruded by Tertiary and Quaternary volcanic and intrusive rocks (Vallier et al., 1994; Beikman, 1994). Sandstone, conglomerate, greywacke, siltstone, and shale with minor associated coals are the predominant sedimentary rocks on the northern peninsula (Detterman and Miller, 1985; Riehle et al., 1987). These sediments were deposited in a fore-arc basin developed during the evolution of the Aleutian arc system (Houston et al., 1993). The prominent Upper Tertiary to Quaternary volcanoes that cap the peninsula are composed chiefly of dacitic and andesitic lava flows, breccias, and tuffs.

Frequent and sometimes radical changes in relative sea level occur in southern Alaska as a result of seismic activity. These changes in sea level have important consequences for coastal geomorphology by causing sudden vertical shifts in wave energy on shorelines and altering patterns of long shore sediment transport (Michel and Hayes, 1994; Mann and Crowell, 1996). Southern Alaska is one of the tectonically most active regions on Earth. The cause of this tectonism is the northward movement of the Pacific plate relative to the North American plate at a rate of 5 to 7 cm/yr (Page et al., 1991). This movement is accommodated by subduction of the Pacific Plate beneath the North American Plate in the Aleutian Trench. Great earthquakes (Mw >= 8) recur at any given plate-boundary segment in southern Alaska about once a century (Jacob, 1986). A recurrence interval of ca. 500-1200 years for great earthquakes is suggested for the region affected by the 1964 Alaskan earthquake (Jacob, 1986; Page et al., 1991; Taber et al., 1991; Mann and Crowell, 1996).

Coastal Geomorphology

Active tectonism, Quaternary volcanism, and glacial erosion have created an intricate, bedrock-delineated coastline along the Gulf of Alaska flank of the Alaska Peninsula in Katmai

National Park and Preserve. In post-glacial times, this coast has been periodically affected by rapid sedimentation caused by volcanic events like the AD 1912 eruption of Novarupta. The bold headland of Cape Nukshak (Figure 2) marks a major boundary in coastal geomorphology. To the northeast, low bedrock points and wave-planed platforms are interspersed with linear sand and gravel beaches fed by glacial outwash streams. Southwest of Cape Nukshak, the coast consists of fjords characteristically headed by broad bayhead deltas built by glacial outwash rivers carrying large loads of volcanic sediments. The Katmai coast, with its combination of rocky, sheltered inner fjords and linear gravel beaches directly exposed to the notoriously rough seas of Shelikof Strait, experiences a wider range of wave energies than does Prince William Sound, Kachemak Bay, or Cook Inlet. Consequently shorelines there show a wider range of geomorphic types than in southern Prince William Sound north of Montague Island. Shoreline terminology follows Michel et al. (1978), Domeracki et al., (1981), and Michel and Hayes (1994).

Exposed bedrock shorelines associated with wave-cut bedrock platforms mantled with locally quarried boulders form rugged headlands such as Cape Nukshak and Cape Douglas and are the most extensive shoreline type on the Katmai coast. Extensive bayhead deltas exist along the coast, nourished by steep-gradient streams descending from rapidly eroding volcanic mountains (Domeracki et al., 1981). Most of these deltas are heavily wave-modified, such as in the head of Dakavak and Katmai Bays. Extensive tidal marshes exist within some bayhead delta systems; one of the largest is in the estuary of the Swikshak River.

Sandy sediments are more abundant on the Katmai coastline than on the southeastern coast of the Kenai Peninsula or in Prince William Sound. Sand sediments form extensive spits and beach ridge plains in bayhead areas along the Katmai coastline. Long-shore transport of sediments is limited to bay interiors except along the coastline between Swikshak and Cape Douglas where glacial outwash feeds vigorous long shore transport of sand and gravels along linearly continuous beaches separated from inland beach ridge plains and marshes by barrier beaches and occasionally by low foredunes. Pocket beaches, an important shoreline type in Prince William Sound, are relatively rare on the Katmai coast, except in sheltered inner fjord settings like Kukak and Amalik Bays. A common shoreline type in Prince William Sound, rocky rubble slopes (Michel and Hayes, 1994), is rare on the Katmai coastline.

Climate in the Northern Gulf of Alaska

During the autumn and winter, storms typically affect the Alaskan coast at intervals of 48 hours or less (Hare and Hay, 1974). The routes taken by storms across the North Pacific are predictable and have consequences for regional climatic patterns. Cyclones generated off the coasts of Siberia and Japan typically track northeastwards, crossing south of the Aleutian Islands towards the coast of North America. Their repeated passages create a region of semi-permanent low pressure, the Aleutian Low (Wilson and Overland, 1986). The Aleutian Low exists approximately 25% of the time, making it an integral part of weather patterns in southern Alaska throughout the year.

Storm frequency and consequently wind intensity in the Gulf of Alaska are greatest between October and April (Overland and Hiester, 1980). In the western gulf, predominate winds are from the west. Winds are typically southerly in the eastern gulf and easterly in the northern gulf (Livingstone and Royer, 1980; Wilson and Overland, 1986). Nearshore winds can be quite variable due to the presence of high mountains that block onshore flow. Along the outer coast of the Kenai Peninsula, storm winds are usually from the southeast. On the shorelines of Shelikof Strait, high winds are more variable in direction, coming from the north down fjords and valleys during times of high pressure in the Bristol Bay region, from the northeast when large cyclones are passing east of Kodiak Island, and from the southwest when large storms move northwards across the Aleutian Island chain to the west.

Storm frequency decreases during the spring in the Gulf of Alaska. Wind speeds also decrease to a low in mid-summer when the East Pacific High is usually strongest. Summer winds are characteristically light except when a storm enters the region (Brower et al., 1977). The Gulf of Alaska is usually cloudy as the result of the frequent passage of storms through the region (Brower et al., 1977). In winter, clouds are generated locally by the flow of cold, interior air out over the warm waters of the gulf. While the East Pacific High is dominant in summer, fog and stratus clouds are frequent in a low-level temperature inversion created over the relatively cool waters of the gulf (Wilson and Overland, 1986).

Precipitation along the southern coast of Alaska is highly variable with a maximum of up to 800 cm/year in the coastal mountains (Royer, 1983) to as little as 59 cm/year at Larsen Bay in

the rainshadow of the mountains of Kodiak Island (Karlstrom, 1969; AEIDC, 1974). Large portions of the coastline between the Copper River delta and the Alaska Peninsula receive 200 cm/year (Royer, 1983). Precipitation away from the coast over the Gulf of Alaska is approximately 100 cm/yr (Wilson and Overland, 1986). Near sea level, most precipitation falls as rain, even in winter (Brower et al., 1977).

Temperatures along the coast of southern Alaska are relatively cool in summer and warm in winter when compared to stations at similar latitudes in the continental interior. Mean annual temperature ranges from 2.2 C at Valdez to 5.4 C at Cape Hinchinbrook. Mean annual precipitation ranges from a low at Larson Bay of 59 cm to 460 cm at Cordova.

Oceanography of Shelikof Strait

Strong, regionally driven ocean currents combined with large-amplitude tides and directionally variable, often high winds create a rapidly changing, storm-wave environment in Shelikof Strait. The Alaska Current is the eastern and polar boundary current of the subarctic gyre in the North Pacific (Royer et al., 1990). It is confined to the deep waters of the Gulf of Alaska about 150 km offshore along the outer shelf break. Its flow is approximately 10 million cubic meters per second, about 1/10 that of the Gulf Stream (Royer, 1989). Warm waters flowing northward in the Alaska Current ameliorate the climate of southern and southeast Alaska. The Alaska Coastal Current (ACC) is a permanent system of near-coastal flow existing shoreward of the Alaska Current between southeastern Alaska and the tip of the Alaska Peninsula (Reed and Schumacher, 1986; Royer et al., 1990). It flows within 40 km of shore and has an average flow of about 200,000 m^3/sec (Royer et al., 1990). Current speeds range from 20 cm/sec in the early summer to 100 cm/sec in the autumn (Reed and Schumacher, 1986). Onshore transport of surface waters by the predominate southerly and easterly winds causes coastal convergence and further concentrates freshwater near the coast. The ACC sweeps southwestwards down Shelikof Strait. In the spring of 1989 it carried *Exxon Valdez* oil with it to the Katmai coast.

Most of the Alaska Coastal Current enters lower Cook Inlet through Kennedy Entrance while a portion of it flows along the eastern side of Kodiak Island, losing velocity and becoming more variable in course. That portion of the ACC entering Cook Inlet moves across the lower

inlet from east to west at velocities up to 40 cm/s (Royer et al., 1990). The current exits the lower inlet along its western margin, entering the western side of Shelikof Strait. The ACC reaches speeds of 60-80 cm/s in Shelikof Strait in autumn. Upon exiting Shelikof Strait, the ACC loses its large freshwater inputs and confining wind stresses. It spreads laterally across the continental shelf and current velocity falls.

Tides in the northwestern Gulf of Alaska are semi-diurnal with a marked inequality between successive low waters. The mean diurnal range varies from 3.2 m at Seward to 4.2 m at Larsen Bay on western Kodiak Island (Wise and Searby, 1977). Maximum daily, spring tide ranges are 2 to 6 m throughout the region, excluding inner Cook Inlet (AEIDC, 1977).

Sea ice is rare in the Gulf of Alaska. Ice forms during winter months in sheltered bays and in areas of large freshwater outflow such as upper Cook Inlet and northwestern Prince William Sound (Brower et al. 1977). Shore ice can occur in fjords on either side of Shelikof Strait.

Waves in the open Gulf of Alaska have a mean significant wave height (mean height of the highest 1/3 of all waves) between 3 and 4 m during the months October through March and decline to between 1 and 2 m in June through August. Maximum significant wave heights reach 7 to 9 m at these same stations (Wilson and Overland, 1986). Open ocean wave heights are >4m for approximately 15% of the time between October and April (Brower et al., 1977). Shelikof Strait is open to storm waves approaching from the southeast and the southwest.

METHODS

Site Selection and Delineation

Study sites were established in 1992 at sites where oil had been consistently observed since 1989 by oil-assessment teams fielded by EXXON and the Alaska Department of Environmental Conservation (Figure 2). Implicit in our research design is the study of the most persistent oil. All sites represent boulder-armored, gravel beaches, most with an underlying bedrock abrasion platform at shallow depth. All these sites received some form of clean-up, ranging from manual removal, rock-wiping, or application of fertilizer, but none were hot-water washed.

In the summer of 1992, permanent sampling transects were established at the five Katmai sites (Appendix A) plus one site on the Kenai Fjords National Park coast (Appendix B). Sampling transects consist of bolt-anchored, tape-measure lines traversing the heaviest concentrations of stranded oil. A 30 x 50 cm quadrat with 5 cm square grids was placed at designated distances along the transect line. Color photographs were then taken of the quadrat frame and the included oiling from as near to a vertical angle as possible. No quantitative, visual assessment of percent oil coverage was made in the field. The plan was to compute oil surface cover using the photographs back in the office. Two oiled sediment samples were taken for chemical analysis from a spot recorded by reference to the oil-transect line. No systematic assessment of subsurface oiling was attempted in 1992.

In August of 1994, we revisited the six study sites established in 1992 and made a number of changes in the methodology to address problems encountered or resulting from 1992 methods. The major changes involved a shift from dependence on photographic methods to in-situ visual discrimination of the extent of oil coverage, and establishment of individually marked quadrats that were placed, as had been the transects, in the zone of heaviest oiling. Individual quadrats, each 40 x 50 cm were positioned over areas of the most extensive and persistent surface oiling. Percent oil cover was independently estimated by three observers. Results were compared and estimates modified until all observers agreed on oil coverage within 5% (Dethier et al., 1993). Making these visual oil-cover estimates involved close scrutiny of the study quadrats both visually and manually. Surface wetness, shadowing, and partial covering by seaweed made careful, nonphotographic assessment of oiling imperative. The position of each quadrat was marked permanently by placing two rock bolts at diagonal corners. Bolt locations were mapped to within +/- 2 cm horizontal distance and +/- 1 cm elevation using an automatic level, tape measure, and stadia rod from a temporary bench mark (tbm) marked by rock bolts on bedrock adjacent to the quadrat swarm.

The quadrat-marking bolts were placed in boulders, and less often in bedrock. Detailed leveling and horizontal mapping of the marker bolts will allow quantification of boulder movements on the study beach during subsequent surveys.

Subsurface oiling was described by observing "dip stones", stones protruding into the substrate near but not within quadrats. These stones were loosened with a five-pound sledge

hammer, then pulled out, and examined for oil clinging to their sides. Dip stones were then reinserted using the sledge hammer. The ideal dip stone was an elongate rock extending vertically below the lowest subsurface oil, because the depth of oiling could be discerned; when oil covered a dip stone to its base, no conclusion could be drawn about maximum depth of oiling. These stones were not randomly selected for two reasons: 1) we did not want to sample within the quadrats, and 2) proper stones are uncommon. On a dip stone, typically the upper extent of oiling was within several cm of the surface, if not at the surface.

Two oiled sediment samples taken from 0-5 cm depth were collected from each site for chemical analysis. Samples were taken where oil was visibly abundant; due to cost of analysis only two samples per site could be collected per visit. A ca. 300 ml sample of mousse was collected using a stainless steel spoon that was rinsed with methylene chloride prior to sampling. Sampling jars (I-Chem) were specially cleaned by the manufacturer. Oil samples were frozen within two hours of their collection.

The sediments of the shorelines studied are covered mainly by gravel, a mixture of particle sizes larger than sand and including boulders. Particle sizes were defined according to the Wentworth scale. Surface oil is described in the following terms:

1. asphalt: heavily oiled sediments held together cohesively in an oil matrix.
2. coat: oil that ranges from 0.1 to 1.0 mm thick and that can be easily scratched off a stone with a fingernail,
3. stain: oil that is < 0.1 mm thick that can not be easily scratched off with a fingernail.

Chemical Analysis of Stranded Oil

The polynuclear aromatic hydrocarbon (PAH) content of samples was determined by a gas-chromatography/mass-spectrometric method at the Auke Bay Laboratory (Short et al., 1996a). The analytes include un-substituted and alkyl-substituted homologues of 2 to 4 ring PAH, and dibenzothiophene homologues (Table 1). PAH were extracted with dichloromethane, purified by alumina/silica gel column chromatography followed by size-exclusion high-performance liquid chromatography. Purified PAH were separated by gas chromatography and measured by mass spectrometry operated in the selected ion monitoring mode. Concentrations of PAH in the dichloromethane extracts were determined by the internal standard method based on

a suite of deuterated-PAH internal standards. Four quality control samples were analyzed with each batch of 12 samples, including 2 reference samples, a method blank, and a method blank spiked with certified hydrocarbon standards obtained from the National Institute of Standards and Technology (NIST). Sample aliquot weights were less than 0.5 g, and most were less than 0.04 g. Method detection limits (MDLs) of PAH were experimentally determined (Glaser et al., 1981), and are reported elsewhere on a mass basis (Short et al., 1996a). The ratio of these mass-based MDLs and sample aliquot weights generally range from 250 - 1,000 ng/g. Analytical accuracy is better than ±15% based on comparison with NIST values, and precision expressed as coefficient of variation usually ranged from 10% to 25%, depending on the PAH analyte.

PAH composition patterns are presented in Figure 3 as mean relative abundances of total PAH (TPAH). Relative abundance for each PAH is determined as the ratio of the hydrocarbon concentration and the TPAH concentration, multiplied by 100. Mean relative abundance is the mean of these ratios for the set of samples specified. Variability of relative abundance for each PAH is presented as the range.

The source of the PAH detected in the samples was evaluated by comparing the relative PAH distribution patterns with patterns derived from experimentally weathered *Exxon Valdez* oil (EVO). A probability distribution has been developed for the least-squares fit of PAH concentrations observed in experimentally weathered EVO samples and corresponding concentrations predicted from a PAH weathering model for EVO based on first-order loss-rate kinetics (Short and Heintz, 1997). Parameters of the EVO weathering model include the PAH proportions of un-weathered EVO, and relative first-order loss-rate constants for 14 selected PAH identified in Table 1. These parameters, together with PAH concentrations determined for environmental samples suspected of contamination by EVO, are used to calculate an error sum-of-squares for the goodness-of-fit of sample PAH with PAH predicted by the EVO weathering model. The probability distribution for the error sum-of-squares is used to estimate the probability that weathered EVO could have the PAH concentrations observed in the environmental sample considered, i.e., a type I error. The EVO weathering model also defines a parameter w_i for the extent of weathering of sample I, which may be used to compare degrees of weathering among samples. This parameter increases from near 0 for unweathered EVO to more positive values as weathering progresses.

RESULTS

Geomorphology of the Study Sites and Their Oiling Conditions in 1994

1) Cape Douglas: Site CD-003A

Located on the outside shoreline of the northern headland enclosing Sukoi Bay (Figure 2; Appendix A: Figure 1) the Cape Douglas site experiences high wave energies from the north, east, and obliquely from the south. The Cape Douglas area is extremely windy, evidenced by groves of prostrate alders and areas of stabilized sand dunes. The study site is located on the upper portion of a broad bedrock platform that merges landward with a boulder-gravel and cobble-pebble ramp rising steeply about 5 m to a 5 to 10 m-wide band of drift logs (Appendix A: Figures 2, 3). The upper, cobble and pebble portion of the ramp is probably highly mobile. However longshore movement of sediment is restricted by the bedrock headlands bordering this section of shoreline.

Oiling in the study site was described as heavy in 1989 (Appendix A: Table 1). In 1990, the oil-impacted area was described as covering an area of 30 x 40 m. Oiling on the SCAT (EXXON's Shoreline Cleanup Advisory Team) segment within which the CD-003A site resides was described as mousse in 1989 and as mousse, tar, coat, and stain in 1990 and 1991 (Appendix A: Table 1). An estimated 844 ft^3 of oil was removed from the larger segment in 1990 and bioremediation fertilizer was applied.

During our visit to CD-003A in 1994, surface oiling was very light and consisted of scattered remnant patches of mousse, tar, coat, and stain plus subsurface mousse. We established 25 permanent quadrats at the CD-003A site in 1994 (Appendix A: Table 2). Oiling in these scattered quadrats ranged from 4 to 45% in cover and consisted mainly of soft asphalt in the interstices of gravel sheltered under the boulder armor. The zone of persistent oiling is near the level of mean high water, inland of the bedrock platform and seaward of the cobble-pebble ramp.

We examined 16 dip stones from around the new quadrats (Appendix A: Table 3). Most of these revealed mousse persisting at depths greater than several centimeters (range 0 - 9 cm). We suspect significant mousse persists at this site to depths > 5 cm.

2) Kiukpalik Island: Site SK-101.

Lying offshore the Katmai coastline and exposed to the waves in Shelikof Strait, the Kiukpalik Island site experiences high wave energies from the northeast and south to southwest (Figure 2; Appendix A: Figure 4). The study site is a bedrock platform, bare at its seaward edge but mantled under a ramp of boulders and cobbles starting near mean high water level and thickening inland (Appendix A: Figure 5). Large granitic boulders up to several meters in diameter form an armor over a substrate of small boulders, cobbles, and pebbles (Appendix A: Figure 6). Freshwater runs across and through the site in several spots. The site is easily located by the lone grove of Sitka spruce trees growing behind it in the meadow.

In 1990, the area of the SK-101 site was described as having medium oiling within an area of 5 x 100 m (Appendix A: Table 1). This oil was described as mousse, tar, coat, and stain. An estimated 1170 ft^3 were removed by cleanup efforts in 1990. In 1994, we described the persisting surface oiling as "very light" and covering an area of approximately 5 x 50 m.

We established 18 permanent quadrats at the SK-101 site in 1994 (Appendix A: Table 4). These quadrats cover the scattered areas of the worst, persistent oiling. Oil cover percentages in these quadrats ranged from 12 to 38% and consisted mainly of coat, asphalt, and stain. All these pockets of remnant oil are located on the cobble-boulder-gravel substrate within and between the large-boulder armor (Appendix A: Figure 7).

We examined 15 dip stones for subsurface oiling (Appendix A: Table 5). Many had bands of tar or asphalt near the surface with mousse at depths > 5 cm. Our impression is that heavy subsurface oiling persists here in the form of only slightly weathered mousse in scattered pockets under the boulder armor.

3) Ninagiak Island: HB-050B

Located in a tiny pocket beach on the south side of Ninagiak Island in Hallo Bay, the HB-050B site experiences high wave energy from Shelikof Strait (Figure 2; Appendix A: Figure 8). This side of Ninagiak Island consists of a high (ca. 10 m), wave-cut platform later dissected by wave erosion to form < 50 m wide pocket beaches filled with a mix of sand, pebbles, cobbles, and boulders. Unconsolidated sediments are locally derived from eroding cliff faces (Appendix A: Figure 9).

At the HB-050B site, an armor of medium to large boulders covers a thin veneer of pebble to boulder gravel over a bedrock platform. The beach profile is relatively low angle (Appendix A: Figures 10, 11), terminating inland at a bedrock cliff. Freshwater seepage is evident on the upper shoreface. It is possible that following certain wave conditions the sand and pebbles from the sea-arch beach to the west may encroach on the study site.

In 1990, oiling around the HB-050B site was described as "medium", covering an area of approximately 5 x 10 m (Appendix A: Table 1). Oiling was mousse, tar, and coat at that time. In 1994, we found the surface oil in the area of HB-050B to be "very light" and to consist of mousse, tar, coat, and stain.

We established 26 quadrats at the Ninagiak site (Appendix A: Table 6). Surface oil cover ranged from 11 to 55% in these quadrats and consisted mainly of asphalt. Eighteen dip stones were examined (Appendix A: Table 7) revealing that mousse persisted in the subsurface. The impression is of scattered patches of remnant, relatively unweathered (i.e., light brown in color and relatively non-viscous) oil mousse.

4) Cape Gull: Site CG-001A.

Located in a west-facing cove north of Cape Gull on the Katmai coast near Kaflia Bay (Figure 2; Appendix A: Figure 12), wave exposure at the Cape Gull site changes radically with tide height. At low tide heights, the site adjoins a low-wave energy lagoon floored by sands, pebbles, and shell fragments. Offshore islets shield the area from waves from Shelikof Strait. During high tides, these protecting islets are reduced greatly in area and the low-tide lagoon is drowned. The study site is partly in the lee of some offshore bedrock outcrops protruding from a bedrock, wave-cut platform thinly mantled by sand-cobble gravel in turn armored by small boulders (Appendix A: Figures 13, 14). The shore is relatively low angle and to the inland terminates in low bedrock cliffs and banks of soil and volcanic ash (Appendix A: Figure 15).

In 1989, the shoreline encompassing our study site was described as heavily oiled (Appendix A: Table 1) in an area 12 x 100 m in size. Oil at that time was described as mousse. Some 14,570 ft^3 were removed from the larger SCAT shoreline segment that includes the CG-001A site. In 1990, surface oiling here was still described as heavy and a further 41 ft^3 were removed that year. In 1994, we found the surface oiling to be very light. However, the portions

of the CG-001A segment lying around the low-tide lagoon south of our quadrats may have been recently buried under a thin blanket of pebble gravel moving onshore and southwards onto the upper shore of the low-tide lagoon. The boulder-armored area where we established our permanent quadrats in 1994 seems unaffected by longshore transport of any kind.

We could find only 12 patches of remnant surface oil suitable for establishment of monitoring quadrats (Appendix A: Table 8). In these 12 quadrats, oil cover ranged from 11 to 30% and was mainly asphalt. Patches of persisting surface oiling were between the boulder armor in the upper intertidal zone.

We examined 19 dip stones from around the CG-001A site (Appendix A: Table 9). Many of these stones failed to reveal subsurface oil. Others revealed mousse up to 7 cm depth. The sporadic occurrence of subsurface oil on the dip stones suggests that the remnant subsurface mousse and tar occurs as widely scattered pockets underneath the surface armor.

5) Kashvik Bay: Site KA-002.

Located on the southern shoreline of outer Kashvik Bay, site KA-002 occupies the upper shoreface of a cobble-boulder beach (Figure 2; Appendix A: Figure 16). Shoreline configuration and wave exposure change markedly according to wave height with a large low-tide lagoon being exposed west of the site during spring tides. The beach profile is low angle (Appendix A: Figure 17), and is backed by a vertical cliff in places and a steep earthen bank in others (Appendix A: Figure 18). Unlike the other five study sites, longshore transport of beach sediments occurs readily in the vicinity of KA-002. There are no bedrock outcrops blocking sediment transport from the east across the upper intertidal zone. Wave energies at high tide water levels are high, though not as high as the Cape Douglas or the Kiukpalik Island sites.

In 1989, oiling at the KA-002 site was described as moderate (Appendix A: Table 1) and covered an area estimated at 20 x 100 m. Cleanup in 1989, 1990, and 1991 removed an estimated 1489 ft^3 of oil. In 1989, oiling at the Kashvik Bay site was described as mousse. In 1990 it was described as mousse, coat, and stain (Appendix A: Table 1). In 1994, we found the surface oiling at KA-002 to be very light across an area of 20 x 100 m and to consist of widely scattered traces of mousse.

During our 1994 visit to KA-002 we were unable to locate any spots for establishing permanent fate and persistence quadrats. Comparing the near-vertical photographs taken along

the transect lines in 1992, we noticed that a large amount of sediment, cobble to small boulder in size, had been brought in by longshore drift from the east. While large boulders composing this beach's armor remained in their 1992 positions, the areas between them had been infilled with smaller sediments (cobbles) sometime between 1992 and 1994. This infilling of newly transported sediment had buried the remaining surface oiling under 20 to 40 cm of unoiled material. Consequently, there is virtually no surface oiling remaining at KA-002. We retained a "very light" descriptor for surface oiling there (Appendix A: Table 1) because of the likelihood that storm waves will sometime exhume the buried surface oil. Several pits dug through the newly deposited sediments at the Kashvik Bay site revealed mousse and tar still present beneath (Appendix A: Figure 19).

PAH Composition of the Stranded Oil

The PAH compositions of all 25 oil samples analyzed are consistent with weathered EVO as the PAH source. Twenty-one of the oil samples analyzed contained concentrations above MDL for all 14 PAH required for application of the EVO weathering model. Type I errors for these 21 samples ranged from 0.11 to 0.90, which means that the PAH distributions of the analyzed samples fit the EVO weathering model better than at least 11% of the experimentally weathered EVO samples, and thereby indicates EVO as a plausible PAH source. The EVO weathering model could not be directly applied to the remaining four of the analyzed oil samples because the chrysenes (3 samples) or C1-phenanthrenes (1 sample) were slightly below MDL. The relative variability (or coefficient of variation) of PAH results increases as concentrations decrease below MDL, so that PAHs that are derived from EVO but include some PAH that are below MDL fit the EVO weathering model less well. Despite the expected poorer fits in these cases, application of the EVO weathering model to the four samples that include PAH results below MDL leads to type I error probabilities that range from 0.07 to 0.37, which indicate EVO as a plausible PAH source for these samples as well.

The PAH concentrations of the samples analyzed confirms their relatively high oil content. Total PAH concentrations (TPAH) range from 0.26 to 4.0 mg TPAH/g sample (Table 2). Weathered EVO contains about 3% TPAH (Marty et al., ms), so these TPAH concentrations are equivalent to oil concentrations that range from about 8 to 130 mg EVO/g sample. These concentrations are consistent with oil contamination that is perceptively obvious.

Most of the samples analyzed were well preserved, in that they had weathered little beyond the initial evaporative weathering that occurred immediately following the *Exxon Valdez* oil spill. Samples of EVO collected from the sea-surface of Prince William Sound 11 days following the oil spill (Short et al., 1996b) contain substantial proportions of naphthalenes and of the less-substituted alkyl-homologues of dibenzothiophene and other PAH (Figure 3A), with values for the weathering parameter w_i that range from 0.26 to 0.98. Proportions of PAH in 22 of the 25 oil samples analyzed are similar (Figure 3B), and have w_i values that range from 0.1 to 2.6 (Table 2), which indicates little additional weathering for these samples compared with the 11 day sea-surface EVO samples. However, w_i values for the remaining 3 oil samples analyzed range from 5.6 to 7.9, which indicates substantial additional weathering, with most of the naphthalenes and the less-substituted alkyl homologues lost (Figure 3C). The TPAH concentrations of these three samples range from 0.26 to 0.36 mg TPAH/g sample, and are among the four lowest TPAH concentrations of the 25 oil samples analyzed.

Mussel and associated sediment samples were taken at Cape Nukshak, on the Katmai National Park coast (Babcock et al., 1996), in 1992 and 1993. The TPAH values for mussel tissue were fairly low, but the one 1992 sediment sample analyzed by GC/MS provided a weathering index of 2.81. This value is similar to the values obtained for the oiled sediment samples taken as part of the oil persistence study (Table 2).

DISCUSSION

Our examination of stranded oil persistence at contaminated sites distant from the origin of the *Exxon Valdez* oil spill combined analysis of geomorphology, physical persistence of the oil, and PAH composition changes in the oil through time. Through this approach, we have attempted to answer the questions initially posed, namely: 1) how long oil contamination persists in worst-case sites, 2) how the PAH composition changed during weathering, and 3) what relationship exists between coastal geomorphology and where stranded oil persists.

The study sites were arrayed along the wilderness coast of Katmai National Park and Preserve, an extensive and ruggedly exposed coast, whose aesthetics and wilderness values were viewed as compromised by the continued presence of oil. Additional concern centered on the possible biological consequences of continued oil contamination of the coast. This coastline is

480-640 km from the origin of the spill, and of the total volume of oil spilled (ca.10.8 million gallons), approximately 2-4% ultimately beached in the Shelikof Strait area (Wolfe el al., 1994). Although a lesser volume of oil arrived on Alaska Peninsula beaches than in Prince William Sound, the areal extent of the oiling was considerable. Much of the oil initially stranded was buried, removed manually, treated with fertilizer, or reduced through weathering processes. By the time this study began in 1992, much of the extensive contamination had become reduced, and study focused on areas of concentrated oiling.

Geomorphology and Oil Persistence

All five sites described here are boulder-armored shorelines that were moderately to heavily oiled in 1989. Boulder-armored shorelines are those where centuries to millennia of wave erosion selectively remove clasts smaller than boulders from the beach surface. The remnant boulder armor is unmoved by the typically occurring wave energies. Consequently, the sediments underlying the boulder armor are seldom disturbed by wave action. Our five study sites are representative of boulder-armored, moderate to high wave energy shorelines throughout the Gulf of Alaska. While superficially cleaned of much of the *Exxon Valdez* oil present in 1989, in 1994 the sites we studied on the Katmai coastline still retained poorly described but significant amounts of subsurface oil (Appendix A: Figure 20).

The persistence of subsurface oil beneath boulder armor on moderate to high wave energy beaches forces a reconsideration of the ecological sensitivity ratings previously applied to Gulf of Alaska shorelines. Vandermeulen (1977), Hayes (1980), Domeracki et al. (1981), and Gundlach et al. (1983) stated that exposed rocky headlands and wave-cut platforms were the shoreline types with the lowest ecological sensitivity to spilled oil due to the short residence time of oil stranded on these types of shorelines (Figure 4). While this is probably true for surface oil, our observations suggest that oil in the subsurface of boulder-armored beaches may be extremely persistent. From observations of the five study beaches since 1989, it is apparent that boulder armor has not been shifted to any significant degree. From weathering pits on the upper surfaces of the boulder armor and from intertidal lichens growing on the boulder armor in protected sites like Cape Gull, it appears that storms capable of moving boulder armors and physically cleaning oil buried in the substrate beneath them may occur only once every century to millennium. We

suggest that boulder-armored beaches have a relatively high ecological sensitivity to spilled oil because of their ability to preserve subsurface oil for long periods.

Alteration of the Oil Composition through Time

Our results are consistent with T/V *Exxon Valdez* oil as the proximate source of the oil found in the analyzed samples. The EVO source is indicated by (a) the concordance of relative PAH abundances in the oil samples with abundances predicted by the EVO weathering model, (b) the high PAH concentrations evident, suggesting the presence of bulk oil, (c) observations that these sample collection areas were heavily contaminated by the oil spilled in 1989 (Schoch, 1993), and (d) the absence of evidence for plausible alternative sources for the PAH found. The consistent presence of chrysenes obviates refined petroleum products as possible alternative PAH sources. Inter- or supratidal petroleum seeps have not been confirmed in the sample collection areas (Becker and Manen, 1989; McGee, 1972), although one near the Cape Douglas area was reported (Miller et al, 1959). An unconfirmed seep is not likely to have caused the broad magnitude of high intertidal oiling studied here. We therefore conclude that EVO is the proximate source of the PAH found in the oil samples analyzed.

The slower progress of weathering we observed in the more oil-contaminated sediments is probably the result of low ratios of surface area to volume of oil contained in these sediments. The thickness of oil films that coat sediment particles tends to increase with sediment oil concentrations, reducing the relative surface area available for weathering processes such as evaporation, dissolution, microbial oxidation, etc., to proceed (Short and Heintz, 1997). As bulk oil concentrations of sediments approach 1%, weathering and biodegradation may proceed slowly, on time scales of years (Owens et al., 1987). Weathering may be further slowed by burial, and by the relatively cold ambient temperatures of the subarctic intertidal. The sediments containing the higher TPAH concentrations we found may therefore persist for decades.

The oil landing on the Katmai coast in 1989 came in the form of mousse, a water-in-oil emulsion with a low surface to volume ratio. As stated above, we expect slower weathering as the surface-to-volume ratio decreases. It is interesting to note that there was little difference in the weathering of 11-day old EVO sampled in Prince William Sound in 1989, and mousse which made its landfall 38-45 days following the spill hundreds of kilometers away. Also, at most sites

where the oil mousse persisted, there was little difference between 1989, 1992 and 1994 oil, and between 11-day-old oil and 5-year-old oil. These observations suggest that mousse can be very recalcitrant to weathering when very little new exposure or disruption of the oil takes place. Thus, as indicated by this study, mousse can be transported long distances and still retain significant concentrations of TPAHs with the potential for toxic effects (Marty et al., 1997).

A somewhat similar case exists with oiled mussel beds in the *Exxon Valdez* spill area, where the byssal threads and sediments underlying the mussels trap oil that also weathers slowly (Babcock et al., 1996). Only one oiled mussel bed was sampled on the Katmai coast, and the weathering index for the 1992 underlying sediment sample was only slightly higher than the values for oiled sediments from this study. Mussel beds occur lower in the intertidal than the boulders harboring persistent oil and so would be exposed to more direct wave action..

Biotic Implications

While the oiling described in this study is not extensive spatially, the small change in PAH abundances in the great majority of the samples (22 of 25), suggests that these sites retain the potential for future contamination. Oil has persisted in all of these sites, in part because they were high in the intertidal, and that height also places them in areas with sparse attached biota, reducing the likelihood of biological effects. It is perhaps more likely that foragers moving through or otherwise using the area (birds, foxes, even bears) could come into contact with the oil and incur some effects, but the oil is generally low in the interstices of the boulders and would therefore be less likely to contact such organisms. Of greater concern, is the potential these sites pose as reservoirs of PAH that may be released more rapidly into the environment in the future if these sediments become more dispersed, e.g., by storm events. Such accelerated release may have adverse effects on adjacent biological resources, such as intertidal organisms.

CONCLUSIONS

Oil has persisted in a relatively unweathered state for five years at sites distant (480-640 km) from the *Exxon Valdez* oil spill. Contrary to previous judgments that oil would have short residence time on exposed rocky shores such as these, the oil has been both persistent and has been slow to weather. The persistence of the oil has been related to its stranding high in the

intertidal on beaches with an armor of large lag boulders. The slowness of the weathering of the oil is related to several factors: 1) it arrived in a somewhat more weathered state than it did in Prince William Sound, 2) its transport as mousse meant that the oil was weathering on its surface but not internally, and 3) it was stranded in geomorphic settings where it was more protected from weathering influences. The transport of oil mousse may allow for the long-distance dispersal of less weathered, and hence, more toxic oil.

The biotic effects of oil persisting along the Katmai coast probably are slight because the oil stranding was initially patchy and persisted ultimately only high in the intertidal of boulder beaches where marine plants and invertebrates are characteristically sparse. However, persistent oiling still has the potential to affect biota if it is released through disturbance of the armoring substrate, e.g., through unusually high-energy wave events.

REFERENCES CITED

AEIDC, NCC (Arctic Environmental Information and Data Center, National Climatic Center) (1977). "Climatic atlas of the continental shelf waters and coastal regions of Alaska". Volume 1: Gulf of Alaska. NOAA RU no. 347, 439 pp.

Alaska Department of Environmental Condervation (1991). "Evaluation of impacted shorelines in the Kodiak/Alaska Peninsula regions. Final Report 1989-1991." ADEC Oil Spill Response Center, Anchorage, AK.

Babcock, M.M., Irvine, G.V., Harris, P.M., Cusick, J.A., Rice, S.D. 1996. Persistence of oiling in mussel beds three and four years after the *Exxon Valdez* oil spill. Pages 286-297 *in* S. D. Rice, R. B. Spies, D. A. Wolfe and B. A. Wright, eds. Proceedings of the *Exxon Valdez* oil spill symposium. American Fisheries Society Symposium 18.

Beikman, H.M. (1994). Geologic Map of Alaska. Plate 1, 1 sheet, scale 1:2,500,000, In: "The Geology of Alaska" (G. Plafker and H.C. Berg, eds.), The Geology of North America, volume G-1, The Geology of Alaska, The Geological Society of America, Boulder, Colorado.

Brower, W.A. Jr., Diaz, H.F., and Pretchtel, A.S. (1977). Marine and Coastal Climatic Atlas. In: Gulf of Alaska, pp. 23-439. "Climatic Atlas of the Outer Continental Shelf Waters and

Coastal Regions of Alaska". Volume 1. Arctic Information and Data Center, University of Alaska, Anchorage.

Dethier, M.N., Graham, S.E., Cohen, S., and Tear, L.M. (1993). Visual versus random-point percent cover estimations: 'objectivity' is not always better. Mar. Ecol. Progr. Ser., 96:93-100.

Detterman, R.L., and Miller, J.W. (1985). Kaguyak Formation - An Upper Cretaceous Flysch Deposit. In: The United States Geological Survey in Alaska: Accomplishments during 1983, edited by S. Bartsch-Winkler and K.M. Reed, pp. 49-51. Circular 945, United States Geological Survey, Washington, D.C.

Domeracki, D.D., Thebeau, L.C., Getter, C.D., Sadd, J.L., and Ruby, C.H. (1981). Sensitivity of coastal environments and wildlife to spilled oil: Alaska, Shelikof Strait Region. Unpublished Report to the National Oceanic and Atmospheric Administration, Outer Continental Shelf Environmental Assessment Program. Published by Research Planning Institute, Inc., Columbia, S.C. 29201.

Glaser, J.A., Forest, D.L., McKee, G.D., Quave, S.A., and Budde, W.L. (1981). Trace analyses for wastewaters. Environ. Sci. Technol. 15:1425-1435.

Gundlach, E.R., Boehm, P.D., Marchand, M., Atlas, R.M., Ward. D.M., and Wolfe, D.A. (1983). The fate of Amoco Cadiz oil. Science 221, 122-129.

Hampton, M. A., Carlson, P.R., Lee, H. J., and Feely, R. A. (1986). Geomorphology, sediment, and sedimentary processes. Pp 93-142. In: "The Gulf of Alaska: Physical Environment and Biological Resources." National Oceanic and Atmospheric Adminstration, United States Department of Commerce, U. S. Government Printing Office, Washington, D.C.

Hare, F.K., and J.E. Hay (1974). The Climate of Canada and Alaska. In: "Climates of North America", edited by R.A. Bryson and F.K. Hare, pp. 49-192. World Survey of Climatology, vol 11, H.E. Landsburg, editor in chief, Elsevier, Amsterdam.

Hayes, M.O. (1986). Oil Spill Vulnerability, Coastal Morphology, and Sedimentation of Outer Kenai Peninsula and Montague Island. In: Outer Continental Shelf Environmental Assessment Program, Final Reports of Principal Investigators, vol 51, December 1986, pp. 419-538. National Oceanic and Atmospheric Administration, Anchorage.

Hayes, M.O., Brown, P.J., and Michel, J. (1977). Coastal geomorphology and sedimentation, Lower Cook Inlet, Alaska. Volume II IN: Trasky,L.L., Flagg, L.B., and Burbank, D.C. (eds)., Environmental Studies of Kachemak Bay and Lower Cook Inlet. Marine/Coastal Habitat Management, Alaska Department of Fish and Game, Anchorage, Alaska, 107 pp.

Hayes, M.O., and Ruby, C.H. (1979). Oil Spill Vulnerability, Coastal Morphology, and Sedimentation of the Kodiak Archipelago. In: Environmental Assessment of the Alaskan Continental Shelf, Final Reports of Principal Investigators, Physical Science Studies, vol 2, December 1979, pp. 1-155. Outer Continental Shelf Environmental Assessment Program, Boulder, Colorado.

Hayes, M.O., Ruby, C.H., Stephen, M.F., and Wilson, S.J. (1976). Geomorphology of the southern coast of Alaska. Proceedings of the 15th Coastal Engineering Conference, Honolulu, Hawaii, pp. 1992-2008.

Houston, W.S., Ethridge, F.G., Warme, J.E., and Gardner, M.H. (1993). Characteristics of lower Tertiary sedimentary rocks along the eastern shore of Katmai National Park, southwest Alaska. Association of American Petroleum Geologis ts National Meeting, New Orleans, April 1993, Abstract.

Jacob, K.H. (1986). Seismicity, tectonics, and geohazards of the Gulf of Alaska region. Pp: 145-184. In: D. W. Hood and S. T. Zimerman (Eds.), "The Gulf of Alaska: Physical Environment and Biological Resources." National Oceanic and Atmospheric Adminstration, United States Department of Commerce, U.S. Government Printing Office, Washington, D.C.

Karlstrom, T.N.V., and Ball, G.E. (1969). "The Kodiak Island Refugium: Its Geology, Flora, Fauna, and History", edited by T.N.V. Karlstrom and G.E. Ball, pp. 20-54. Boreal Institute, University of Alberta, Edmonton.

Livingstone, D., and Royer, T.C. (1980). Observed surface winds at Middleton Island, Gulf of Alaska and their influence on the ocean circulation. Journal of Physical Oceanography 10, 753-

Mann, D.H., and Crowell, A.L. (1996). A large earthquake occurring 700-800 years ago in Aialik Bay, southern coast Alaska. Can. J. Earth Sci. 33:117-126.

Mann, D.H., and Peteet, D.M. (1994). Extent and timing of the last glacial maximum in southwest Alaska. Quaternary Research 42, 136-148.

Marty, G.D., Short, J.W., Dambach, D.M., Willits, N.H., Heintz, R.A., Rice, S.D., Stegemann, J.J., Hinton, D.E. (1997). Ascites, premature emergence, increased gonadal cell apoptosis, and cytochrome-P450IA induction in pink salmon larvae continuously exposed to oil-contaminated gravel during development. Canadian Journal of Zoology (in press).

Michel, J., and Hayes, M.O. (1993a). Evaluation of the condition of Prince William Sound shorelines following the Exxon Valdez oil spill and subsequent shoreline treatment: Volume I: 1991 geomorphological shoreline monitoring survey. National Oceanic and Atmospheric Administration Technical Memorandum NOS ORCA 67. 94 pp.

Michel, J., and Hayes, M.O. (1993b). Evaluation of the condition of Prince William Sound shorelines following the Exxon Valdez oil spill and subsequent shoreline treatment: Volume I: Summary of results - geomorphological shoreline monitoring survey of the Exxon Valdez spill site, Prince William Sound, Alaska, September 1989 - August 1992. National Oceanic and Atmospheric Administration Technical Memorandum NOS ORCA 73.

Michel, J., and Hayes, M.O. (1994). Geomorphological shoreline monitoring of the Exxon Valdez spill site, Prince William Sound, Alaska, July 1994. National Oceanic and Atmospheric Administration Technical Memorandum NOS ORCA 82.

Michel, J., and Hayes, M.O. (1996). Evaluation of the condition of Prince William Sound Shorelines following the Exxon Valdez oil spill and subsequent shoreline treatment. Volume II: 1994 Geomorphological Monitoring Survey, July 1994. NOAA Technical Memorandum NOS ORCA 91.

Michel, J., Hayes, M.O., and Brown, P.J. (1978). Application of an oil vulnerability index to the shoreline of lower Cook Inlet, Alaska. Environmental Geology 2, 107-117.

National Research Council (1985). "Oil in the Sea: Inputs, Fates, and Effects." National Academy of Sciences Press, Washington, D.C., 601 pp.

Overland, J.E., and Hiester, T.R. (1980). Development of a Synoptic Climatology for the Northeast Gulf of Alaska. Journal of Applied Meteorology 19, 1-14.

Owens, E.H., Harper, J.R., Robson, W., and Boehm, P.D. (1987). Fate and persistence of crude oil stranded on a sheltered beach. Arctic 40(Suppl. 1): 109-123.

Page, R.A., Biswas, N.N., Lahr, J. C. and Pulpan, H. (1991). Seismicity of continental Alaska. In: Neotectonics of North America. Edited by D.B. Slemmons, E. R. Engdahl, M.D. Zoback, and D.D. Blackwell. Geological Society of America. Decade Map Volume 1, Boulder Colorado. Pp. 47-68.

Payne, J.R., Kirstein, B.E., McNabb, G.D., Jr., Lambach, J.C., De Oliveira, C, Jordan, R.E., and Hom, W. (1983). Multivariate analysis of petroleum hydrocarbon weathering in the subarctic marine environment. In: Proc. 1983 Oil Spill Conf., Publ. No. 4356, American Petroleum Institute, Washington, D.C. pp:423-434.

Plafker, G. (1969). The Alaska earthquake, regional effects, tectonics. U.S. Geological Survey Professional Paper 543-I, 74 pp.

Reed, R.K., and Schumacher, J.D. (1986). Physical Oceanography. In: "The Gulf of Alaska: Physical Environment and Biological Resources", edited by D.W. Hood and S.T. Zimmerman, pp. 57-75. National Oceanic and Atmospheric Administration, Washington, D.C.

Riehle, J.R., Detterman, R.L., Yount, M.E., and Miller, J.W. (1987). Preliminary Geologic Map of the Mt. Katmai Quadrangle and Portions of the Afognak and Nanek Quadrangles, Alaska, Open File Report 87-593, U.S. Geological Survey, Washington, D.C.

Royer, T.C. (1982). Coastal Fresh Water Discharge in the Northeast Pacific. Journal of Geophysical Research 87C: 2017-2021.

Royer, T.C. (1983). Northern Gulf of Alaska. Review of Geophysics and Space Physics 21:1153-1155.

Royer, T.C. (1989). Alaskan Oil Spill. Science 245:243. (letter).

Royer, T.C., Vermersch, J.A., Weingartner, T.J., Niebauer, H.J., and Muench, R.D. (1990). Ocean Circulation influencing the Exxon Valdez oil spill. Oceanography : 3-10.

Royer, T.C., Hansen, D.V., and Pashinski, D.J. (1979). Coastal Flow in the northern Gulf of Alaska as observed by dynamic topography and satellite-tracked drogued drift buoys. Journal of Physical Oceanography 9:785-801.

Schoch, C. (1994). Geomorphological shoreline classification and habitat sensitivity atlas for Katmai National Park and Preserve, Alaska. Conference Proceedings, The Coast: Organizing for the Future, The Coastal Society, Fourteenth International Conference, April 17-21, Charleston, S.C. p. 291- 294 (extended abstract).

Short, J.W, Heintz, R.A. (1997). Identification of *Exxon Valdez* oil in sediments and tissues from Prince William Sound and the northwestern Gulf of Alaska based on a PAH weathering model. Environmental Science and Technology (in press).

Short, J.W., Jackson, T.J., Larsen, M.L., and Wade T.L. (1996). Analytical methods used for the analysis of hydrocarbons in crude oil, tissues, sediments, and seawater collected for the Natural Resources Damage Assessment of the *Exxon Valdez* oil spill. American Fisheries Society Symposium 18:140-148.

Short, J.W., Sale, D.M., and Gibeaut, J.C. (1996). Nearshore transport of hydrocarbons and sediments after the *Exxon Valdez* oil spill. American Fisheries Society Symposium 18:40-60.

Taber, J.J., Billington, S., and Engdahl, E.R. (1991). Seismicity of the Aleutian arc. In: Neotectonics of North America. Edited by D. B. Slemmons, E. R. Engdahl, M. D. Zoback, and D.D. Blackwell. Geological Society of America. Decade Map Volume 1, Boulder, Colorado. Pp 47-68.

Terada, K., and Hanzawa, M. (1984). Climate of the North Pacific Ocean. In "Climates of the Oceans" (H. Van Loon, ed.), pp. 431-504. Elsevier, Amsterdam.

Vallier, T.L., Scholl, D.W., Fisher, M.A., Bruns, T.R., Wilson, F.H., von Huene, R., and Stevenson, A.J. (1994). Geologic framework of the Aleutian arc, Alaska. In "The Geology of Alaska" (G. Plafker and H.C. Berg, Eds.), p. 367-388. DNAG volume G-1, Geological Society of America, Boulder, Co.

Vandermeulen, J.H. (1977). The Chedabucto Bay spill, Arrow 1970. Oceanus 20, 32-39.

Wilson, J.G., and Overland, J.E. (1986). Meteorology, In: "The Gulf of Alaska: Physical Environment and Biological Resources", edited by D.W. Hood and S. T. Zimmerman, pp. 31-54. National Oceanic and Atmospheric Administration, Washington, D.C.

Wise, J.L., and Searby, H.W. (1977). Selected Topics in Marine and Coastal Climatology. In: Gulf of Alaska, pp. 7-22. "Climatic Atlas of the Outer Continental Shelf Waters and

Coastal Regions of Alaska", Volume 1. Arctic Information and Data Center, University of Alaska, Anchorage.

Table 1.-- Polynuclear aromatic hydrocarbons (PAHs) measured for this study. Asterisk indicates PAHs used in the EVO weathering model (Short and Heintz) to evaluate EVO as the PAH source. Abbreviations are given for the most abundant of the analyzed PAH in weathered EVO, and are used in Figure 3.

PAHs	Abbreviation	PAHs	Abbreviation
Naphthalene	Naph	*C-2 Phenanthrene/Anthracenes	C2phenan
2-Methylnaphthalene	Menaph2	*C-3 Phenanthrene/Anthracenes	C3phenan
1-Methylnaphthalene	Menaph1	*C-4 Phenanthrene/Anthracenes	C4phenan
Biphenyl	Biphenyl	Fluoranthene	
C-2 Naphthalenes	C2naph	Pyrene	
Acenaphthylene		C-1 Fluoranthene/Pyrenes	C1fluora
Acenaphthene		Benz-a-anthracene	
*C-3 Naphthalenes	C3naph	*Chrysene	Chrysene
*C-4 Naphthalenes	C4naph	*C-1 Chrysenes	C1chrys
Fluorene	Fluorene	*C-2 Chrysenes	C2chrys
C-1 Fluorenes	C1fluor	C-3 Chrysenes	C3chrys
*C-2 Fluorenes	C2fluor	C-4 Chrysenes	C4chrys
*C-3 Fluorenes	C3fluor	Benzo-b-fluoranthene	
Dibenzothiophene	Dithio	Benzo-k-fluoranthene	
*C-1 Dibenzothiophenes	C1dithio	Benzo-e-pyrene	
*C-2 Dibenzothiophenes	C2dithio	Benzo-a-pyrene	
*C-3 Dibenzothiophenes	C3dithio	Perylene	
*Phenanthrene	Phenanth	Indeno[1,2,3-cd]pyrene	
Anthracene	Anthra	Dibenzo-a,h-anthracene	
*C-1 Phenanthrene/Anthracenes	C1phenan	Benzo-ghi-perylene	

Table 2.-- Total PAH (TPAH) concentrations and weathering parameter (w) values for oil samples collected for this study. Concentrations for TPAH are given as mg TPAH/g dry sample weight. Weathering parameter values are dimensionless (Short and Heintz), with increasing values corresponding to greater weathering. Respective results for TPAH and w are separated by a comma for duplicate analyses.

Location	Collection Date	TPAH (mg/g)	Weathering parameter, w
Cape Douglas	30 Jul 92	0.515, 0.832	1.44, 1.05
	06 Aug 94	3.52, 3.43	1.82, 2.02
Cape Gull	02 Oct 89	3.20	0.114
	02 Aug 92	0.260, 0.291	5.90, 7.86
	10 Aug 94	0.341, 0.364	2.02, 5.56
Kashvik Bay	04 Aug 92	0.577, 4.00	1.12, 0.486
	11 Aug 94	1.81, 3.09	0.844, 0.468
Kiupalik Is.	31 Jul 92	1.24, 2.80	0.739, 0.464
	08 Aug 94	2.84, 2.75	1.49, 1.53
Cape Kubugakli	29 Sep 89	2.83	1.93
McArthur Pass	27 May 94	0.513, 1.99	2.45, 2.67
Ninagiak Is.	10 Dec 89	2.99	1.58
	01 Aug 92	1.09, 2.21	1.42, 0.637
	09 Aug 94	2.12, 2.37	1.39, 0.817

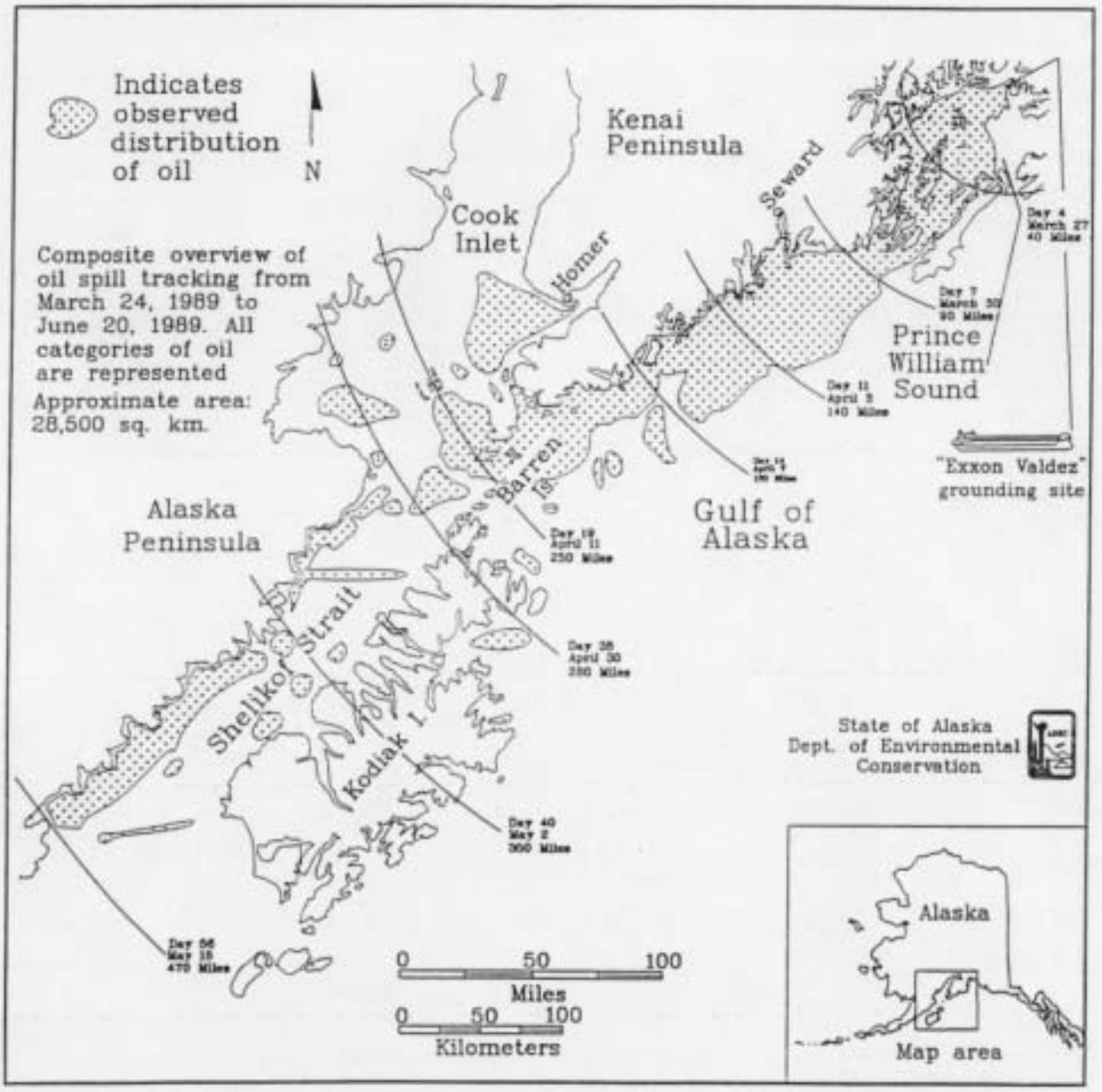

Figure 1. Geographical extent of the Exxon Valdez oil spill through time (March 24, 1989-June 20, 1989). Figure courtesy of the State of Alaska, Department of Environmental Conservation.

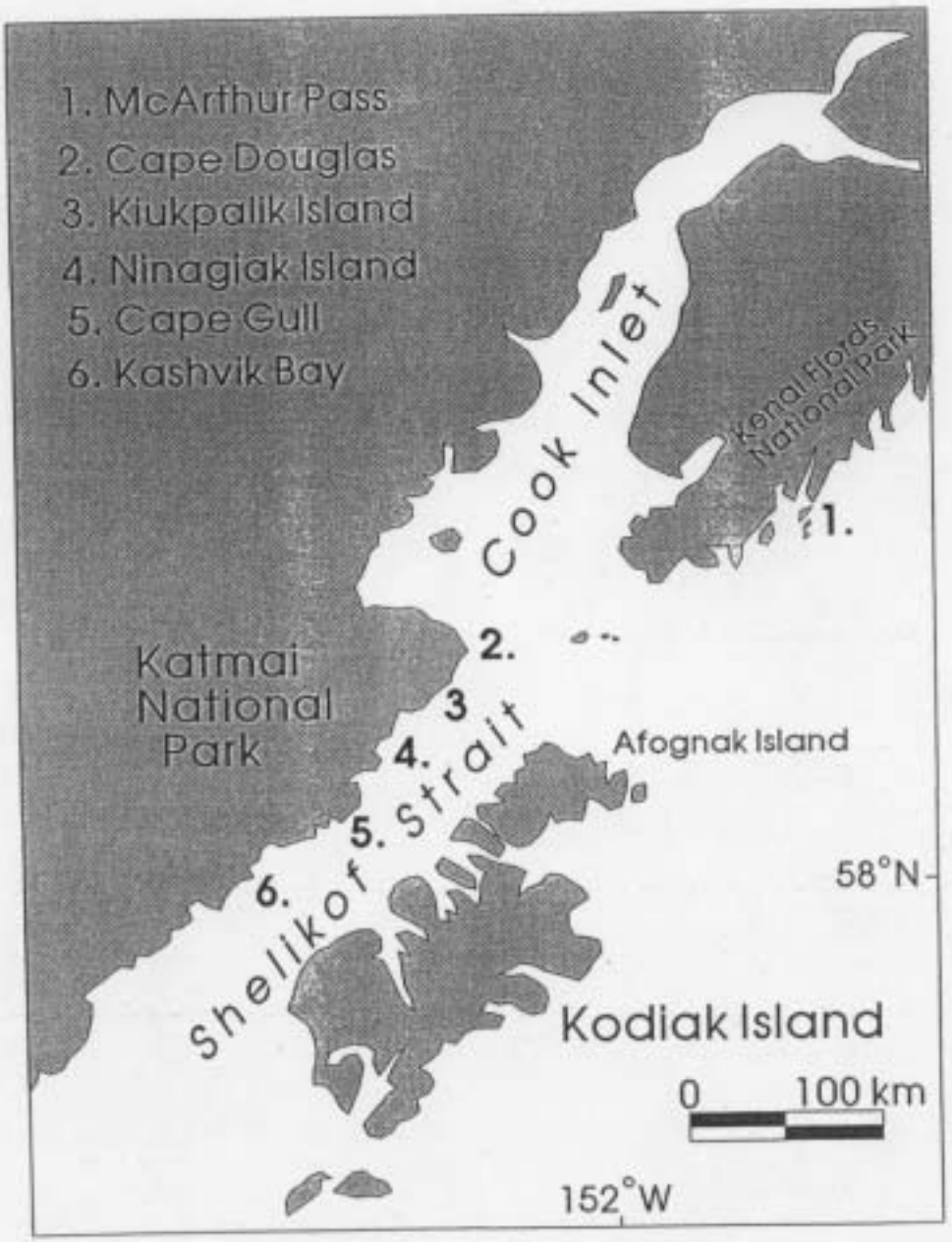

Figure 2. Location map for the oil persistence study sites.

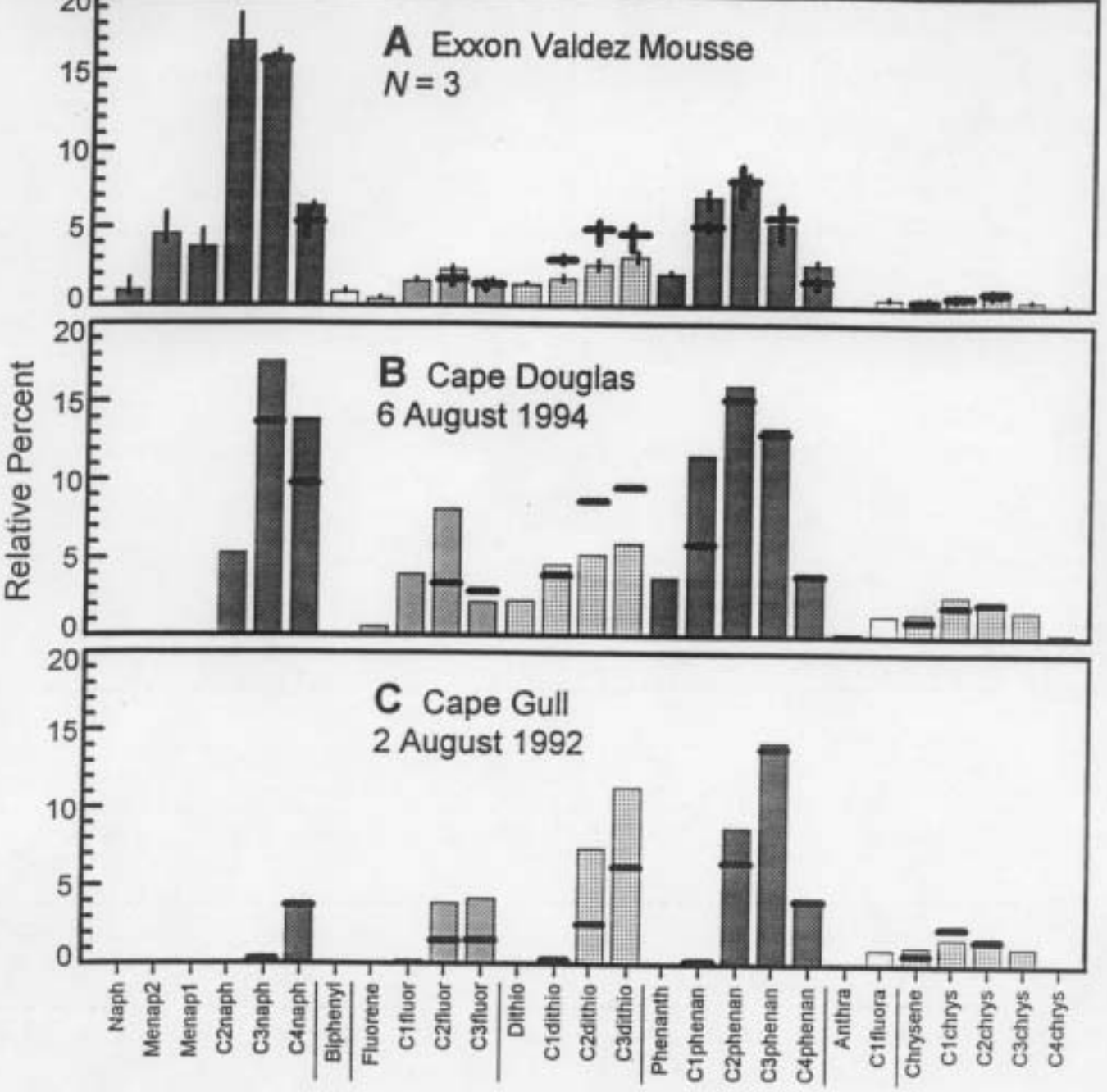

Figure 3. Relative PAH abundances in Exxon Valdez mousse oil and in typical oilsamplesanalyzed for this study. Vertical bars indicate ranges, and horizontal bars indicate abundances predicted by the EVO weathering model used to assess EVO as the source of the PAHs detected (3). The significance of differences between predicted and observed abundances is given by the type I error (see text). (A) Exxon Valdez mousse oil collected 11 days following the oil spill of 24 March 1989 in Prince William Sound (6), (B) oil in sediments collected from Cape Douglas on 4 Aug 94 and typical of 22 of the 25 oil samples analyzed for this study, (C) the most weathered (w_t = 7.86) oil in sediment collected for this study, from Cape Gull on 2 Aug 92.

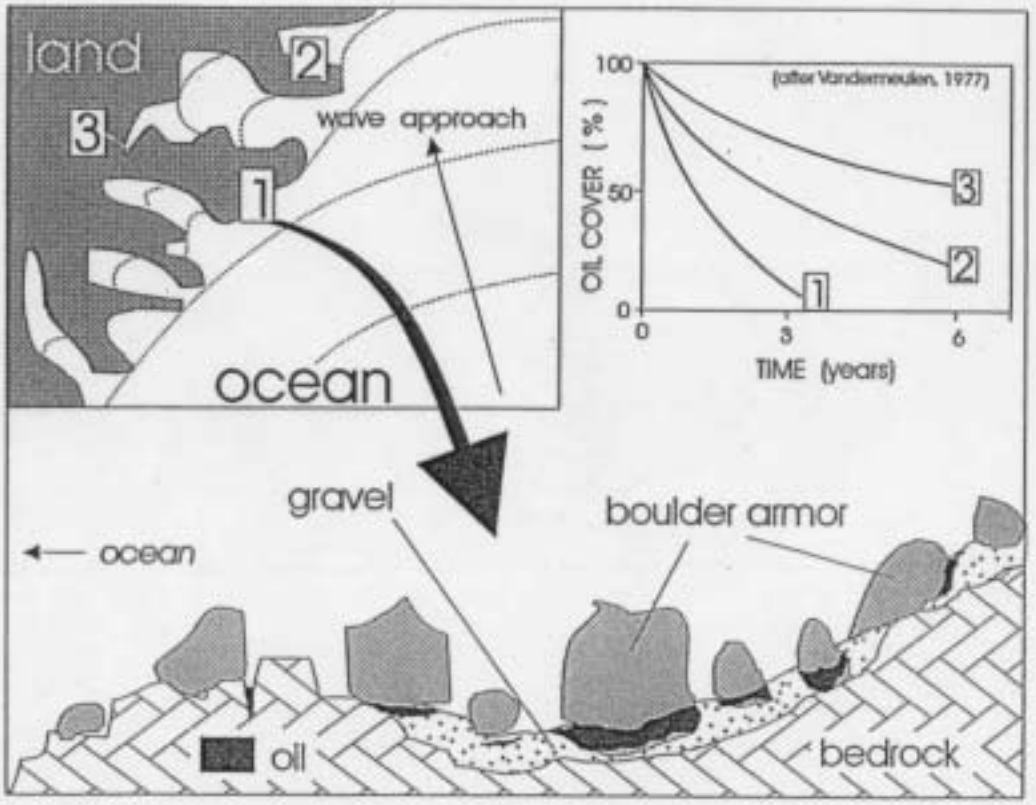

Figure 4. Surface oil persists longest on beaches with lower wave energies (upper two figures). However, results of the present study show that this may not be true for subsurface oil. Where a boulder armor protects gravel substrate from wave erosion, subsurface oil persists for years, despite high wave energies.

APPENDIX A

SUPPLEMENTAL INFORMATION FOR KATMAI NATIONAL PARK SITES

APPENDIX A

Table of Contents

APPENDIX A

SUPPLEMENTAL INFORMATION FOR KATMAI NATIONAL PARK SITES

Introduction

More detailed supplementary information for the study sites along the Katmai National Park coast is provided in this Appendix. Also provided is additional information regarding methods changes between 1992 and 1994.

Methods

Re-evaluation of the Methodology Used in the 1992 Fate and Persistence Survey

All oil-cover data collected during the initial year of this study in 1992 relied on the analysis of photographs taken of quadrats placed along transect lines. Detailed inspection of the 1992 photographs while in the field in 1994 convinced us that it was impossible to accurately estimate oil percent cover from them. Shadows cast by boulders, especially on sunny days, obscured the extent of oil patches. Wet surfaces and pieces of seaweed compounded the problem. We conclude that photography is only dependable for assaying oil coverage on flat, unshadowed rock surfaces. Unfortunately, oiling of flat bedrock surfaces is rare at our study sites. Careful on-site inspection, assisted by touch and much neck craning, is the only dependable way to estimate percent oil cover at bouldery, interstice-rich sites. Consequently, we discarded the results of the 1992 survey, retaining only general descriptions of oiling amount and chemical data from subsurface samples of mousse

Tables and Figures: Attached

APPENDIX TABLE 1. Oiling conditions reported at the study sites in Katmai National Park and Preserve.

Cape Douglas, Segment CD 003A

	Referring to the Study Area Within Larger Exxon Segment						Referring to Whole Segment				
Date	*ADEC Oil Category*	*Exxon Oil Category*	*Impacted Area "wide" (m)*	*Impacted Area "moderate" (m)*	*Impacted Area "narrow" (m)*	*Impacted Area "very light" (m)*	*Length Oiled x Width Oiled (m)*	*Meters Treated*	*Amount Oil Removed $(ft)^3$*	*Fertilizer Applied (pounds)*	*Type of Oil**
9/22/89	heavy	heavy							0	0	m
4/27/90			40 x 30					110	844	3	m,t,c,s
5/22/91							70 x 20	14	4		m,t,c,s
8/6/94		very light				25 x 5					m,t,c,s

Kiupalik Island, Segment SK 101

	Referring to the Study Area Within Larger Exxon Segment						Referring to Whole Segment				
Date	*ADEC Oil Category*	*Exxon Oil Category*	*Impacted Area "wide" (m)*	*Impacted Area "moderate" (m)*	*Impacted Area "narrow" (m)*	*Impacted Area "very light" (m)*	*Length Oiled x Width Oiled (m)*	*Meters Treated*	*Amount Oil Removed $(ft)^3$*	*Fertilizer Applied (pounds)*	*Type of Oil*
4/25/90		medium		100 x 5				100	1170	10	m,t,c,s
5/24/91							425 x 59	10	3.5		m,t,c,s
8/8/94		very light				50 x 5					m,t,c,s

Ninagiak Island, Segment HB 050B

	Referring to the Study Area Within Larger Exxon Segment						Referring to Whole Segment				
Date	*ADEC Oil Category*	*Exxon Oil Category*	*Impacted Area "wide" (m)*	*Impacted Area "moderate" (m)*	*Impacted Area "narrow" (m)*	*Impacted Area "very light" (m)*	*Length Oiled x Width Oiled (m)*	*Meters Treated*	*Amount Oil Removed $(ft)^3$*	*Fertilizer Applied (pounds)*	*Type of Oil*
4/25/90		medium		10 x 5							m,c,s
5/23/92							30 x 7	10	2		m,t,c,s
8/9/94		very light				10 x 5					m,t,c,s

APPENDIX TABLE 1 (continued)

Kaflia Bay, Cape Gull, Segment K 0922-CG 001

	Referring to the Study Area Within Larger Exxon Segment						Referring to Whole Segment				
Date	*ADEC Oil Category*	*Exxon Oil Category*	*Impacted Area "wide" (m)*	*Impacted Area "moderate" (m)*	*Impacted Area "narrow" (m)*	*Impacted Area "very light" (m)*	*Length Oiled x Width Oiled (m)*	*Meters Treated*	*Amount Oil Removed $(ft)^3$*	*Fertilizer Applied (pounds)*	*Type of Oil*
9/30/89	heavy	heavy						1401	14,567	0	m
4/21/90		heavy	100 x 12				1300 x (<3-6 m)	10	40.5	0	m,c,s
8/10/94		very light				50 x 3					m

Kashvik Bay, Segment KA 002

	Referring to the Study Area Within Larger Exxon Segment						Referring to Whole Segment				
Date	*ADEC Oil Category*	*Exxon Oil Category*	*Impacted Area "wide" (m)*	*Impacted Area "moderate" (m)*	*Impacted Area "narrow" (m)*	*Impacted Area "very light" (m)*	*Length Oiled x Width Oiled (m)*	*Meters Treated*	*Amount Oil Removed $(ft)^3$*	*Fertilizer Applied (pounds)*	*Type of Oil*
9/29/89	moderate	moderate						600	765	0	m
4/29/90		very light				100 x 20	1600 x (<3 m)	100	719	0	m,c,s
							80 x 11	100	5		m
8/11/94		very light				100 x 20					m

Type of oil: m = mousse, t = tar, c = coat, s = stain.

1989 descriptive terms
heavy = > 9 m wide or > 50% cover
moderate = < 6 m wide or 10% to 50% cover
light = < 3 m wide or < 10% cover
very light = intermittent oil in form of splatters, stains, and tarballs

1990 descriptive terms
wide = > 6 m wide and > 50 % cover
moderate = > 6m wide and < 50% cover
narrow = < 3 m wide and > 10% cover
very light = < 10% cover regardless of width

TABLE 2. Oil Cover and Quadrat Arrangement at the Cape Douglas Fate and Persistence Monitoring Site, Segment CD003a, 8/7/94

Quadrat	% Oil Cover	Oil Description	Relative Elevations of Marker Bolts (cm)[a]	Bearing from Bench Mark (degrees)[b]	Distance from Bench Mark (m)	Distances to Other Bolts (m)[c]	Quadrat's Long-axis Orientation (degrees)
A	12	soft asphalt with embedded fines, rainbow and grey sheening	181	90	6.32	to B = 3.91	85
B	20	coat, stain, soft asphalt with embedded fines, grey sheen	170	59	7.59	to C = 3.69	90
C	20	coat, soft asphalt, rainbow sheen	193.5	54	3.96	to D = 3.93	145
D	45	interstitial mousse, soft asphalt with embedded fines, grey sheen	155.5	27.5	6.96	to E = 1.59	11
E	45	interstitial mousse, soft asphalt with embedded fines, grey sheen, coat, stain	153.5	15	7.18	to F = 0.74	35
F	20	interstitial mousse, soft asphalt with embedded fines, grey sheen	137.5	10.5	6.74	to G = 1.32	90
G	15	coat, grey sheen	147	9	5.55	to H = 1.09	125
H	45	interstitial asphalt, interstitial mousse	174	8.5	4.52	to I = 1.46	25
I	35	coat, thick interstitial mousse, soft asphalt with embedded fines, grey sheen	175	359	3.58	to J = 1.67	125
J	20	coat	168	345	4.19	to K = 2.87	94
K	16	coat	160	354	6.88	to L = 1.52	150
L	40	interstitial asphalt, coat	152.5	348	8.62	to M = 0.48	162
M	40	coat, interstitial asphalt, rainbow sheen	158	350.5	8.19	to N = 3.20 to O = 2.92	162
N	13	interstitial asphalt with embedded fines, coat	117.5	353	11.27	to O = 1.50	320
O	15	interstitial asphalt, rainbow and grey sheen	129	58	10.78		59

TABLE2. (continued)

Quadrat	% Oil Cover	Oil Description	Relative Elevations of Marker Bolts (cm)[a]	Bearing from Bench Mark (degrees)[b]	Distance from Bench Mark (m)	Distances to Other Bolts (m)[c]	Quadrat's Long-axis Orientation (degrees)
P	8	interstitial tar, coat	152.5	346.5	7.33	to L = 0.80	222
Q	19	coat, stain, interstitial tar, grey sheen, interstitial mousse	166	339	7.61	to P = 1.05 to R = 2.03	238
R	12	coat, interstitial tar	154	333	6.09	to S = 1.23	58
S	20	interstitial tar, coat, rainbow sheen, interstitial mousse	174	328.5	7.19	to T = 0.76	22
T	16	interstitial mousse, rainbow sheen	150.5	324.5	7.64	to U = 1.89	360
U	12	interstitial tar	143	320	9.37	to V = 1.59	304
V	20	interstitial tar, coat	130.5	327	10.30		55
W	9	interstitial mousse and tar	144	303.5	11.36	to U = 3.69 to X = 2.11	96
X	8	coat	143	299.5	9.35	to Y = 4.80	49
Y	4	interstitial tar	172.5	273.5	10.85 [c]		131

[a] Stadia rod is set on top of bolt. These altitudes are relative to one another.
[b] Bearings are relative to magnetic north. While internally consistent, all these bearings may be ± 2 degrees off of magnetic north. When reoccupying this site, check at least two bolts before setting magnetic north on the instrument.
[c] tape line bends over intervening boulders

TABLE 3. Subsurface Oiling Described under Randomly Selected "Dip-Stones" at the Cape Douglas Fate and Persistence Monitoring Site, Segment CD003a, 8/7/94

Stone Number	Location	Description of Oiling
1	25 cm from edge of quadrat A	mousse to -2 cm depth in substrate
2	quadrat C	0 to -3 cm mousse penetration
3	30 cm outside quadrat D	mousse penetrates to depth of 1-3 cm below surface
4	edge of quadrat E	mousse extends 2 to 3 cm below surface
5	50 cm from quadrat H	penetration by mousse to 3-5 cm below surface
6	edge of quadrat I	penetration by mousse to 6-7 cm below surface
7	edge of quadrat J	2 clean dip stones
8	quadrat K	clean dip stone
9	quadrat L	mousse to at least 8 cm along edge of stone
10	quadrat M	mousse to at least 8 cm along edge of stone
11	quadrat N	penetration by mousse to > 5 cm
12	between quadrates P and Q	penetration by mousse to 9 cm, no oil on another dip stone
13	1 m south of quadrat T	mousee penetration to 1 cm on one stone, to 2.5 cm on a second
14	within 1 m of edge of quadrat U	penetration by mousse to 3+, 2.5, and 1.5 cm
15	border of quadrat V	mousse penration to 5-7 cm
16	25 cm outside quadrat X	clean dip stone

TABLE 4. Oil Cover and Quadrat Arrangement at the Kiukpalik Island Fate and Persistence Monitoring Site, Segment SK 101, 8/10/94

Quadrat	% Oil Cover	Oil Description	Relative Elevations of Marker Bolts (cm)	Bearing from Bench Mark (degrees) [b]	Distance from Bench Mark (m)	Distances to Other Bolts (m)	Quadrat's Long-axis Orientation (degrees)
A	28	coat with embedded spruce needles	301.5	8.5	12.42	to Q = 0.60 to B = 3.23	346
B	28	coat with embedded spruce needles, interstitial tar	273	10	9.24	to C = 2.25	87
C	20	coat, stain, interstitial tar and mousse	309.5	359	10.42	to D = 1.90	324
D	38	stain, coat with ebedded spruce needles, interstitial tar	304.5	358.5	8.84	to E = 1.21	49
E	38	interstitial tar and mousse, stain, coat	305.5	353	7.62	to F = 0.23 to G = 0.68	278
F	30	stain, coat, interstitial tar	297.5	352	7.45	to H = 3.48 [c]	345
G	17	coat, stain, interstitial tar and mousse, grey sheen	301.0	346	7.27	to H = 1.14 [c]	330
H	58	coat, stain, interstitial mousse and tar	285.0	339.5	6.65	to I = 3.71 [c] to J = 2.36 to K = 7.41 to P = 2.16 [c]	38
I	36	stain, coat	248.5	10	4.51		5
J	<15		471.5	321.5	5.33		316
K	14	coat, interstitial tar and mousse	489.5	278.5	7.83	to L/M = 1.98	296
L [a]	36	coat, interstitial tar and mousse	492.5	266.5	8.44		19
M [a]	<15		492.5	266.5	8.44		267
N	12	coat, interstitial tar	507	269	9.61	to L/M = 1.29 [c]	360
O	16	coat, interstitial tar and mousse	304.5	207	16.87	to L/M = 14.60	324
P	35	coat with spruce needles embedded	221.0	32	2.84		354
Q	16	coat with spruce needles embedded	305.0	9.5	12.98		8

TABLE4.(continued)

Quadrat	% Oil Cover	Oil Description	Relative Elevations of Marker Bolts (cm)	Bearing from Bench Mark (degrees) [b]	Distance from Bench Mark (m)	Distances to Other Bolts (m)	Quadrat's Long-axis Orientation (degrees)
R	12	stain, coat, interstitial tar and mousse	310.5	214	17.48	to L/M = 14.14 to O = 2.09 to bench mark = 17.59	326

[a] marked by a shared bolt

[b] relative to magnetic north. While internally consistent, all these bearings may be ± 2 degrees off of magnetic north.

[c] tape line bends over intervening boulders

TABLE 5. Subsurface Oiling Described under Randomly Selected "Dip-Stones" at the Kiupalik Island Fate and Persistence Monitoring Site, Segment SK 101, 8/8/94

Stone Number	Location	Description of Oiling
1	edge of quadrat A	clean to 10+ cm depth
2	30 cm north of quadrat C	1) clean to 10 cm depth 2) clean to 2+ cm depth 3) clean to 3+ cm depth
3	30 cm west of quadrat B	clean to 5 cm depth
4	1 m north of quadrat C	oil to 7+ cm depth
5	1 m north of quadrat F	down flanks of stone: 1 cm of coat, 1 cm of asphalt, 9+ cm of mousse
6	30cm outside of quadrat H	coat and mousse to a depth of 3 cm
7	between quadrates G and H	1 cm of tar above 4+ cm of mousse
8	30 cm east of quadrat I	clean to 5+ cm depth
9	1 m south of quadrat I	3 cm of coat above 1 cm of mousse
10	east of quadrat K	1) 4 cm of tar above 4+ cm of mousse
11		2) 3 cm of tar above 8+ cm of mousse
12	near quadrates L and M	1) 2+ cm of asphalt 2) 2.5+ cm of asphalt
13	20 cm north of quadrat N	1 cm of tar above 7+ cm of mousse
14	20 cm east of quadrat R	2 cm of tar over 6+ cm of mousse
15	50 cm southeast of quadrat O	3 cm of tar over 8+ cm of mousse
16	75 cm northwest of O	1 cm of tar over 4+ cm of mousse

TABLE6. Oil Cover and Quadrat Arrangement at Ninagiak Island Fate and Persistence Monitoring Site, Segment HB 050B, 8/9/94

Quadrat	% Oil Cover	Oil Description	Relative Elevations of Marker Bolts (cm)	Bearing from Bench Mark (degrees) [b]	Distance from Bench Mark (m) [c]	Distances to Other Bolts (cm)	Quadrat's Long-axis Orientation (degrees)
A	37	asphalt with embedded pebbles	278.5	310	8.60	to B = 64	262
B	55	asphalt with embedded pebbles, brown mousse with rainbow sheen	288.5	307.5	9.14 [e]	to C = 109	20
C	45	asphalt, brown mousse with rainbow sheen	284.5	300.5	9.01 [e]	to D = 74	31
D	30	brown mousse, asphalt with embedded pebbles	286.5	299	9.67 [e]	to E = 52	20
E	28	tar with embedded pebbles	282.5	296	9.70 [e]	to O = 344.5 [e] to O = 344.5 [e] to N = 430	305
F	21	asphalt	305	305	12.30 [e]	to E = 315 [e]	38
G	12	asphalt with embedded pebbles	310.5	306	13.98 [e]	to W = 242 to V = 405 [e]	332
H	27	asphalt with embedded pebbles	302.5	300.5	12.32 [e]	to E = 274 to F = 111.5 to G = 218 [e]	330
I	28	asphalt with embedded pebbles	313	298	12.56 [e]	to E = 291 to H =55	265
J	17	asphalt withh embedded pebbles	345	287	14.87		354
K	17	asphalt with embedded pebbles	357.5	285	14.12	to S = 214	264
L	23	asphalt with embedded pebbles and cobbles	347.5	288	13.36	to J =152 to K = 106	333
M	28	asphalt with embedded pebbles and cobbles	350	287	13.00	to L = 41	252
N	25	asphalt with embedded pebbles and cobbles	347	282	12.98	to K = 129 to M = 166 [e] to L = 139	334
O	23	asphalt with embedded pebbles	349	285	12.38		278

TABLE 6 ,(continued)

Quadrat	% Oil Cover	Oil Description	Relative Elevations of Marker Bolts (cm)	Bearing from Bench Mark (degrees) [b]	Distance from Bench Mark (m)[c]	Distances to Other Bolts (cm)	Quadrat's Long-axis Orientation (degrees)
P	11	asphalt with embedded pebbles and cobbles	336	281.5	10.88	to Q = 89.5	264
Q	13	asphalt with embedded pebbles and cobbles	338	278	11.41	to R = 113	288
R	37	asphalt with embedded pebbles and cobbles	348.5	278	12.52	to N = 101	262
S	23	asphalt with embedded pebbles and cobbles	385	277	14.97	to U = 306.5 [c]	246
T	9	asphalt with embedded pebbles and cobbles	355.5	267	13.84	to U = 296 [c] to R = 292 [c]	248
U	14	asphalt with embedded pebbles, rainbow sheen	378.5	268.5	16.69		230
V	26	asphalt with embedded pebbles	285	314	17.26	to X = 468 [c] to Y = 642 [c] to Z = 666 [c]	322
W	11	asphalt with embedded pebbles and cobbles	287.5	312	15.72	to V = 168	285
X	25	asphalt with embedded pebbles and cobbles	290	304.5	20.61		289
Y	18	asphalt with embedded pebbles and cobbles	289	304	22.32	to X = 179 [c] to Z = 156	240
Z	16	asphalt with embedded pebbles and cobbles	290.5	301	22.49		362

[a] Stadia rod is set on top of bolt. These altitudes are relative to one another.
[b] relative to magnetic north. While internally consistent, all these bearings may be about 6 degrees off of magnetic north due to disturbance of the setup by a passerby.
[c] tape line bends over intervening boulders

TABLE 7. Subsurface Oiling Described under Randomly Selected "Dip-Stones" at Ninagiak Island, Segment HB 050B

Stone Number	Location	Description of Oiling
1	1 m northeast of quadrat A	no oil to -10 cm
2	75 cm west of quadrat A	no oil 0-3 cm, 1+ cm mousse
3	50 cm south of quadrat D	2 cm coat, 5 cm mousse
4	1.5 m south of quadrat D	no oil to 3 cm depth
5	2 m south of quadrat E	1 cm asphalt, 3 - 5 cm mousse
6	2 m south of quadrateE	4 cm tar, 3+ cm of mousse
7	at quadrat P	3 cm mousse
8	at quadrat O	2 - 7 cm mousse
9	between quadrates N and K	1 cm asphalt, 6 cm mousse, 2+ cm without oil
10	1 m south of quadrat L	no oil to -8 cm
11	2 m west of quadrat J	1 cm asphalt, 5+ cm of mousse
12	at quadrat S	no oil to -5 cm
13	1 m west of quadrat S	no oil to -5 cm
14	1.5 m south of quadrat T	1 cm asphalt, 5 cm mousse, 4 cm no oil
15	1.5 m southeast of quadrat T	1 cm no oil, 1 cm asphalt, 2 cm mousse, 5+ cm clean
16	1 m east of quadrat T	3+ cm mousse
17	near quadrat Z	no oil to -11 cm
18	1.5 m south of quadrat Z	1 cm no oil, 7 cm mousse, 5+ cm clean

TABLE 8. Oil Cover and Quadrat Arrangement at the Cape Gull Fate and Persistence Monitoring Site, Segment Kaflia Bay, Cape Gull, Segment K 0922-CG 001, 8/10/94

Quadrat	% Oil Cover	Oil Description	Relative Elevations of Marker Bolts (cm)	Bearing from Bench Mark (degrees) [a]	Distance from Bench Mark (m)	Distances to Other Bolts (m)	Quadrat's Long-axis Orientation (degrees)
A	11	hard asphalt with embedded shells and pebbles	166.0	10.0	27.80	to B = 6.97	29
B	24	hard asphalt with embedded shells and pebbles	176.5	13.0	21.00	to C = 0.96	315
C	11	hard asphalt with embedded shells and pebbles	170.5	13.0	20.09	to D = 12.93	321
D	18	hard asphalt with embedded shells and pebbles	171.5	33.5	8.08	to H = 6.37	75
E	12	hard asphalt with embedded shells and pebbles	198.0	55.5	13.96	to D = 7.15 to G = 8.40	274
F	15	hard asphalt with embedded shells and pebbles	191.5	89.0	8.59	to G = 1.28	2
G	30	hard asphalt with embedded shells and pebbles	172.0	85.0	7.44	to H = 2.48	92
H	14	hard asphalt with embedded shells and pebbles	194.0	84.5	5.25	to I = 1.49	112
I	12	hard asphalt with embedded shells and pebbles	205.5	101.0	5.21 [b]		26
J	14	hard asphalt with embedded shells and pebbles	202.5	104.0	3.25 [b]	to H = 2.55	71
K	18	hard asphalt with embedded shells and pebbles	186.5	130.5	3.14 [b]	to J = 1.53	332
L	14	hard asphalt with embedded shells and pebbles	215.5	159.0	5.98 [b]	to K = 3.59	9

[a] tape line bends over intervening boulders

[b] relative to magnetic north. While internally consistent, all these bearings may be ± 2 degrees off of magnetic north

TABLE 9. Subsurface Oiling Described under Randomly Selected "Dip-Stones" at the Cape Gull Fate and Persistence Monitoring Site, Segment Kaflia Bay, Cape Gull, Segment K 0922-CG 001, 8/10/94

Stone Number	Location	Description of Oiling
1-3	1 m north of quadrat A	1) clean to 3+ cm depth 2) 50% of stone circomference covered to depth of -3 to -5 cm with asphalt 3) clean to a depth of 6+ cm
4	1 m north of quadrat B	mousse to 7 cm depth on stone
5-6	1.5 m west of quadrat B	1) clean to 5+ cm depth 2) clean to 10+ cm depth
7	2 m northwest of quadrat B	clean to 6+ cm depth
8	2 m east of quadrat E	clean to 11+ cm depth
9	3 m north of quadrat E	clean to 5+ cm depth
10	2 m west of quadrat E	1 to 3 cm depth is covered in mousse
11	1 m west of quadrat H	1/3 of stone's circumference is covered with 1 to 3m thick mousse
12	edge of quadrat G	0 - 1 cm depth is clean, 3 to 9 cm depth is mousse-covered, below 9 cm depth is clean
13	1 m northwest of quadrat F	clean to 4+ cm depth
14	1.5 m west of quadrat F	2 cm of asphalt over 3 cm of mousse clinging to stone
15-17	1.5 m south of quadrat L	1) clean to 4+ cm depth 2) clean to 3+ cm depth 3) clean to 8+ cm depth
18	1 m north of quadrat L	clean to 2+ cm depth
19	1 m west of quadrat L	clean to 3+ cm depth

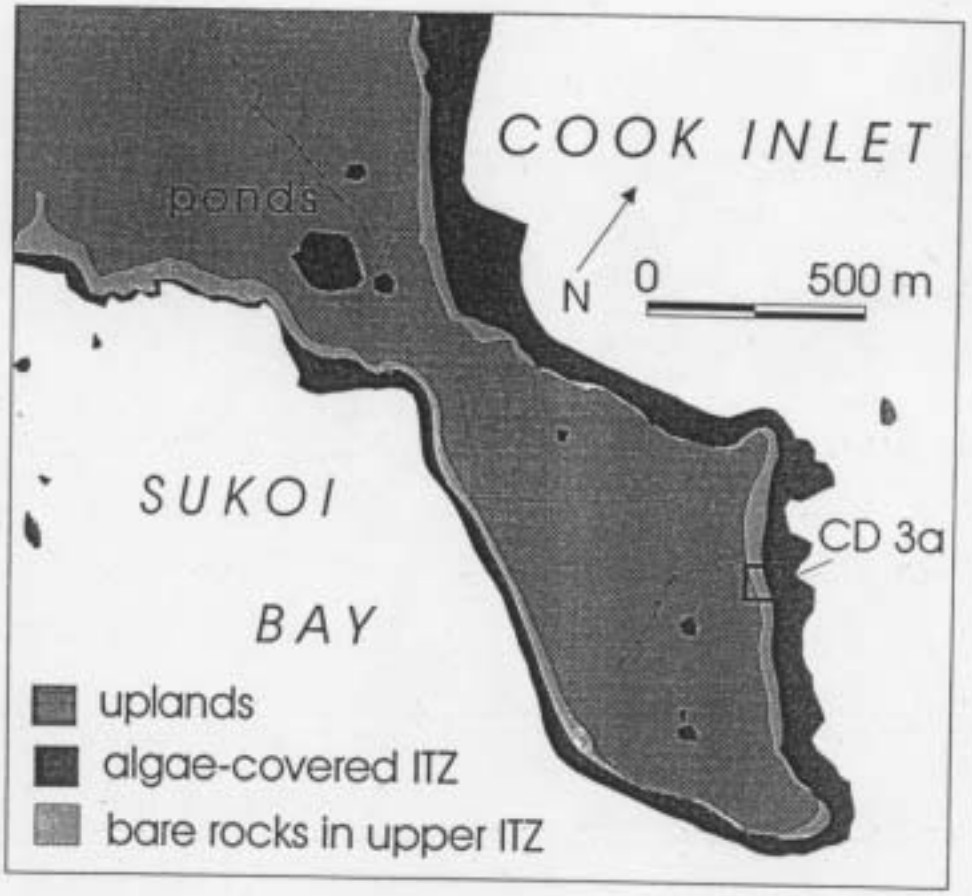

Figure 1. Location of the CD-3 site in the Cape Douglas area of Katmai National Park and Preserve. From a 1:2000 vertical aerial photograph taken at low spring tide.

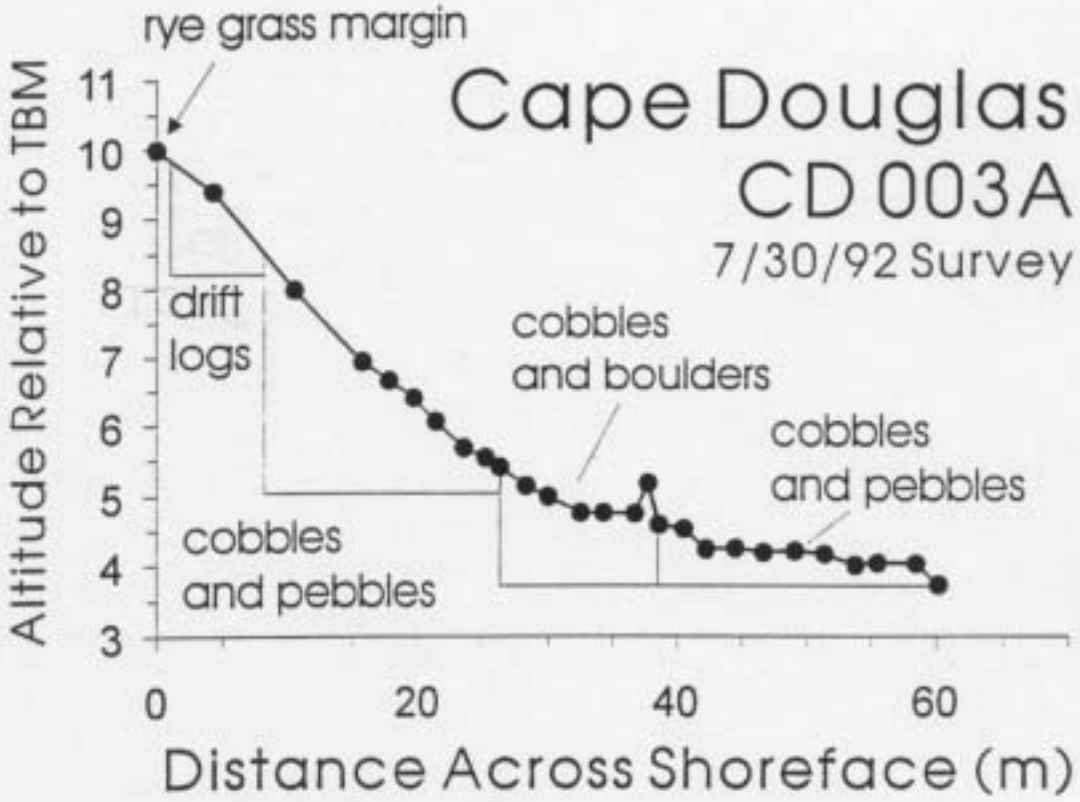

Figure 2. Leveling transect perpendicular to the shore showing the beach profile at the Cape Douglas study site.

Figure 3. The Cape Douglas site (CD-003A) in August 1994. The tape measures shown here were laid out in an attempt to reoccupy the 1992 survey lines. Under the new monitoring scheme, a temporary bench mark was established atop the bedrock outcrop in the left middle distance. Permanent quadrat locations were then marked with rock bolts at different distances and bearings from this bench mark.

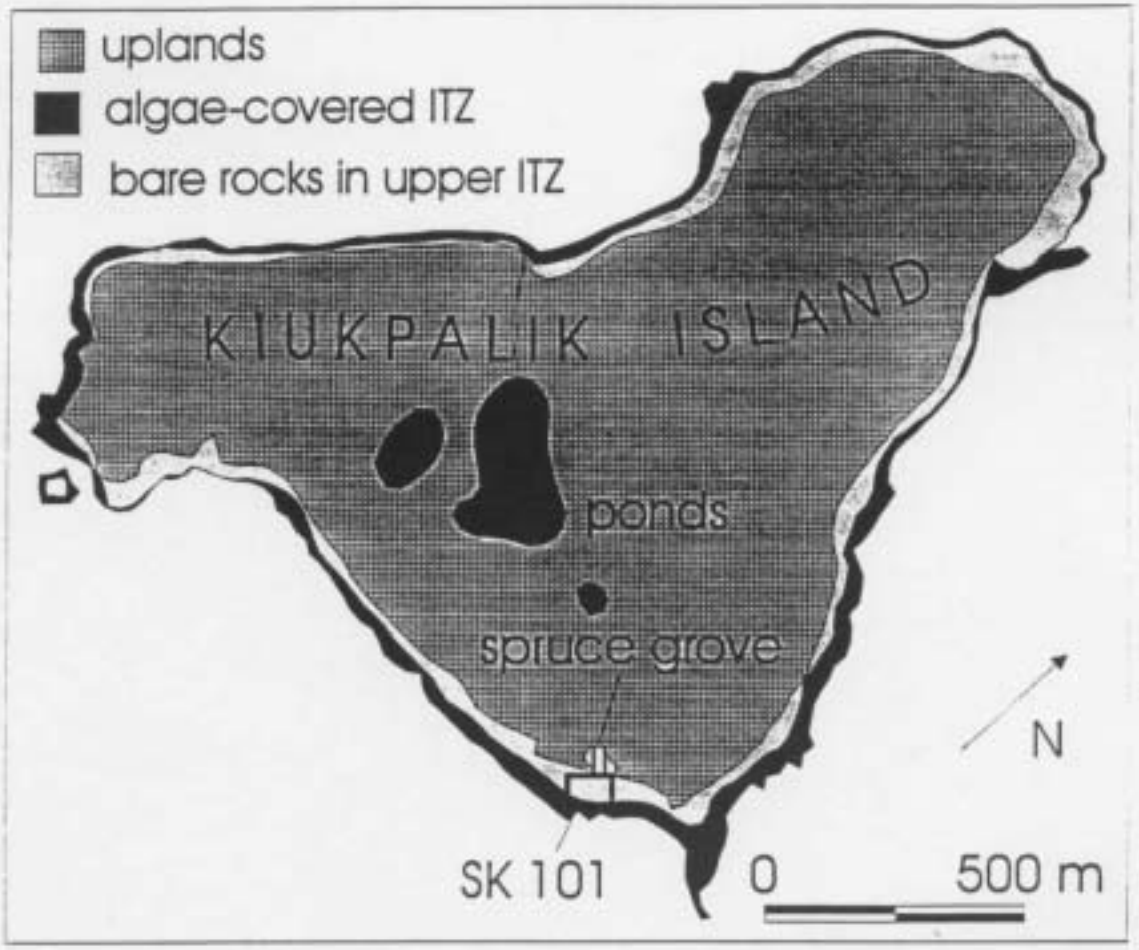

Figure 4. Kiukpalik Island, Shelikof Strait coastline of Katmai National Park and Preserve showing location of the fate and persistence study site on the southeast shore.

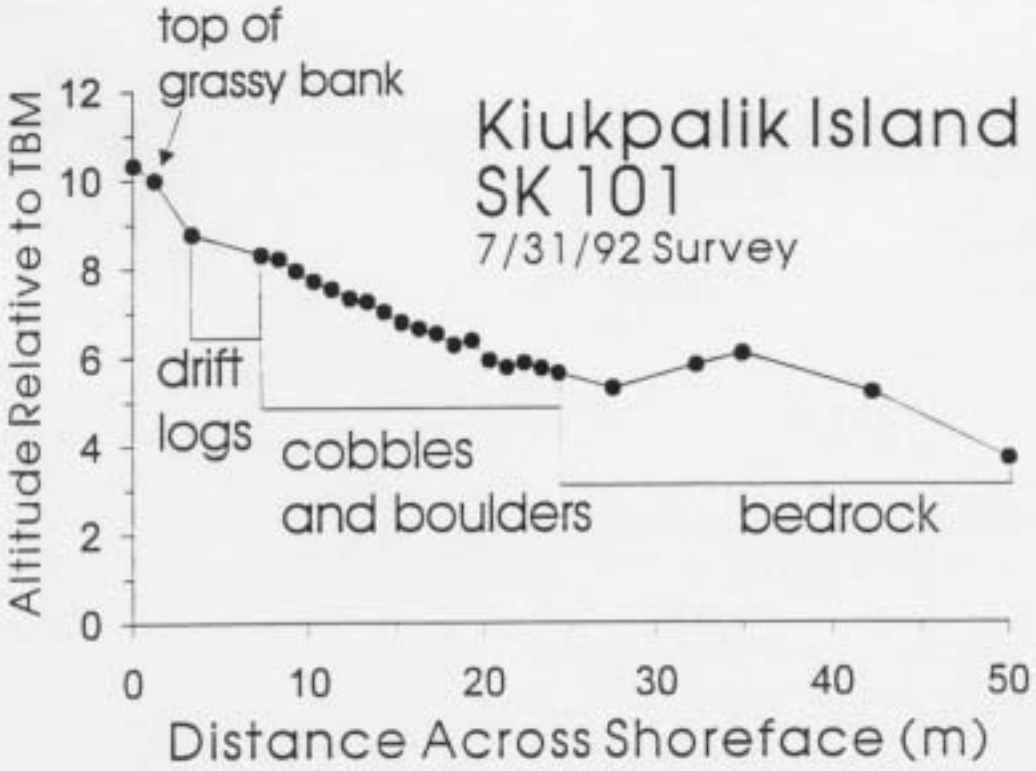

Figure 5. Leveling profile perpendicular to the shore across the SK-101 site on Kiukpalik Island.

Figure 6. The Kiukpalik Island site (SK-101) in August 1994 looking up and across the upper shoreface to the autolevel in place over a temporary bench mark. The spruce grove is out of sight off the right side of this photograph. Remnant oil is between the large boulders armoring this beach.

Figure 7. Sketch plan-view map of the Kiukpalik Island study site showing main substrate characteristics and approximate locations of quadrates emplaced in 1994.

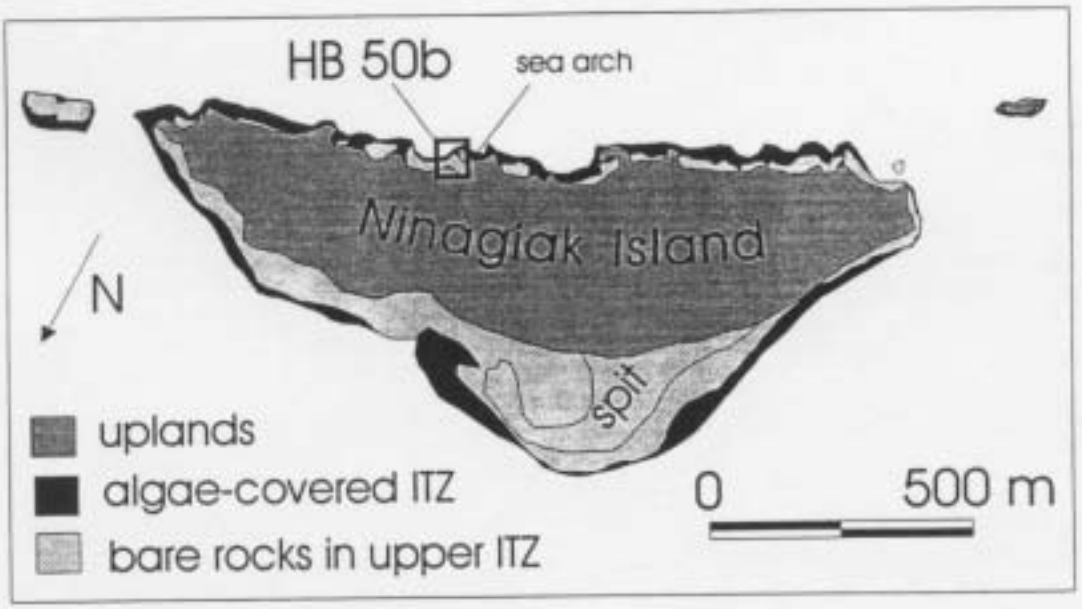

Figure 8. Ninagiak Island, Hallo Bay, Shelikof Strait coastline of Katmai National Park and Preserve. The study site is on the southern side of the island in a small pocket beach. Redrawn from a 1:2000 vertical aerial photograph taken at low spring tide.

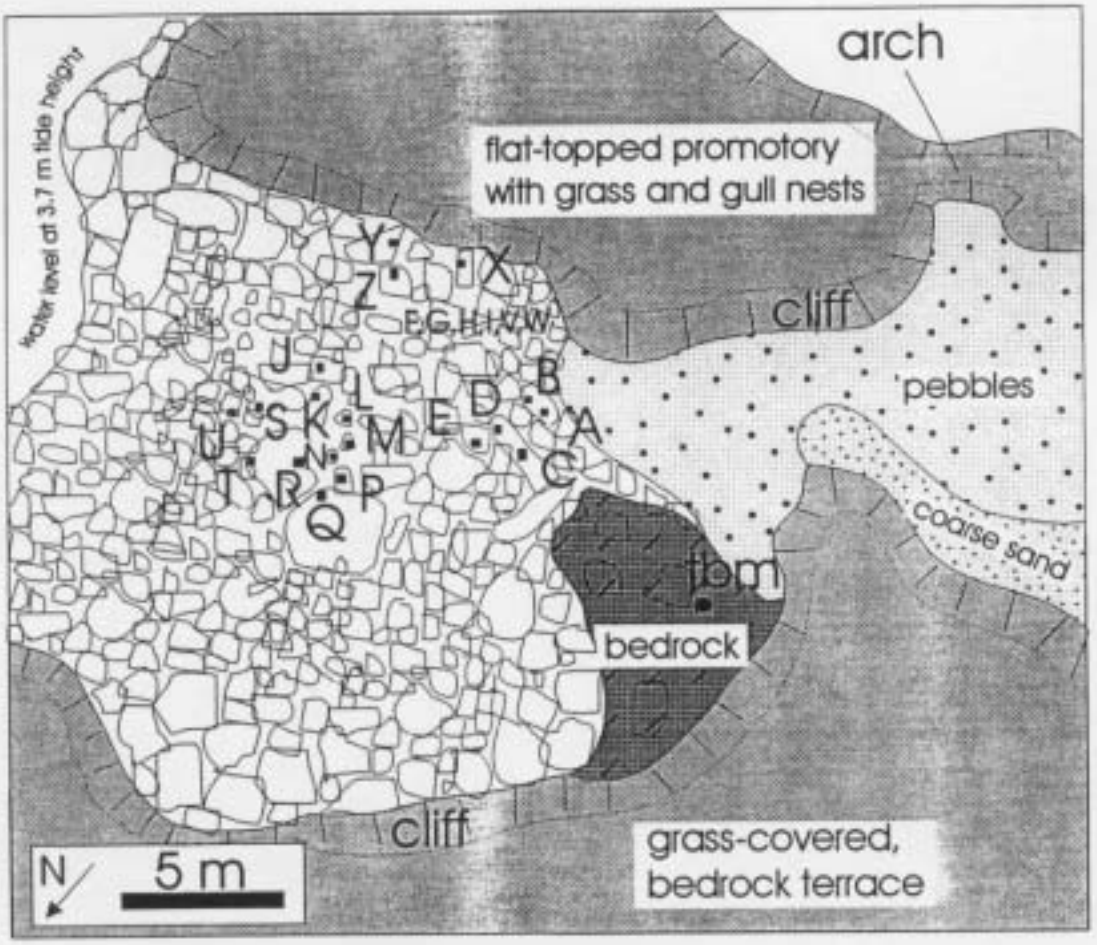

Figure 9. Sketch plan-view map of the Ninagiak Island study site showing main substrate characteristics and approximate locations of 1994 quadrates.

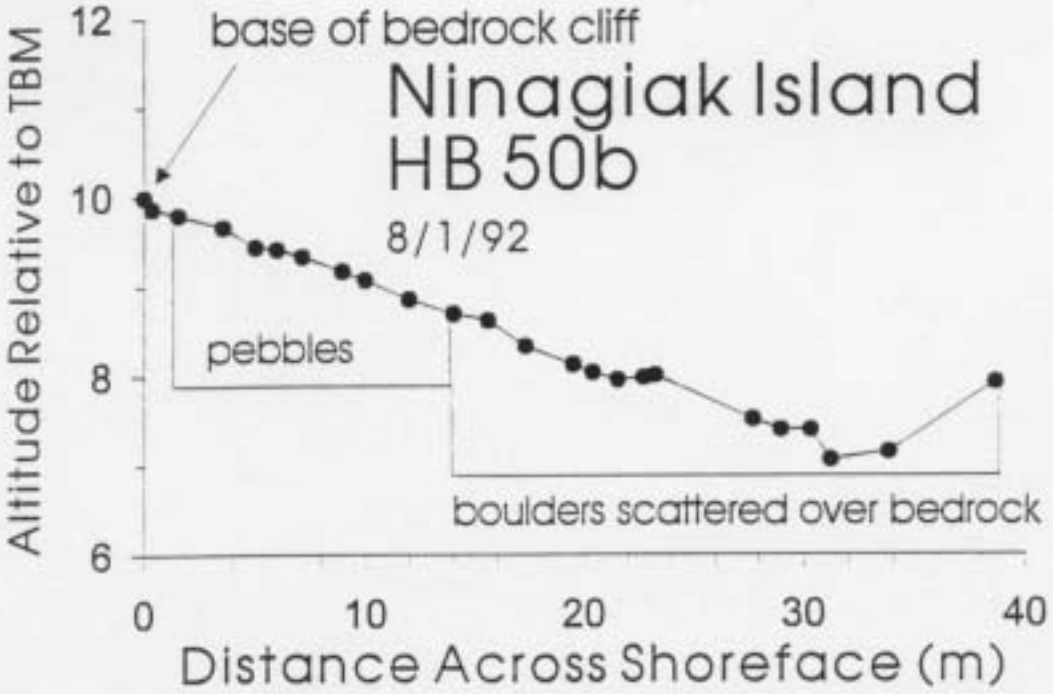

Figure 10. Leveling profile perpendicular to the shore across the HB-50b site on Ninagiak Island.

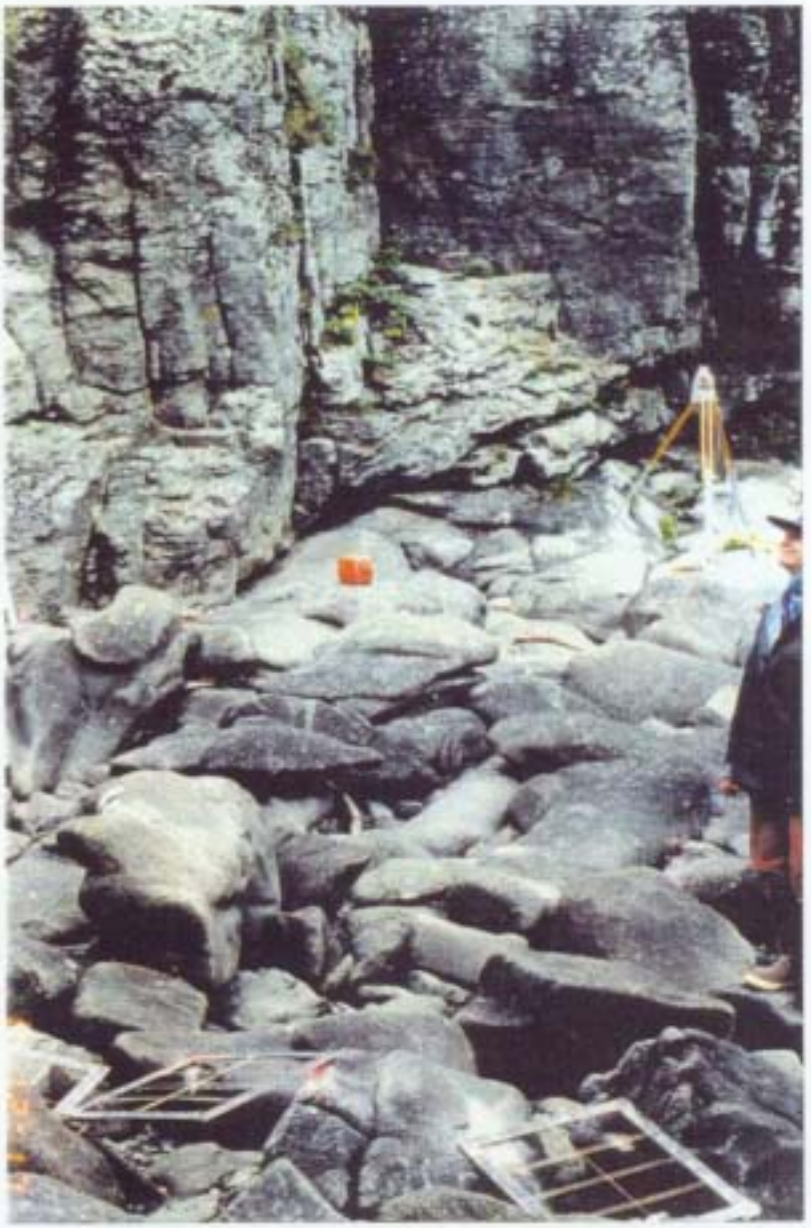

Figure 11. The Ninagiak Island site (HB-050B) in August 1994 showing the autolevel positioned over a temporary benchmark established on bedrock at the base of the sea cliff enclosing much of this pocket beach. Quadrat frames are shown in position, diagonal corners marked with rock bolts. At this site, the boulder armor comprises a thin cover over bedrock.

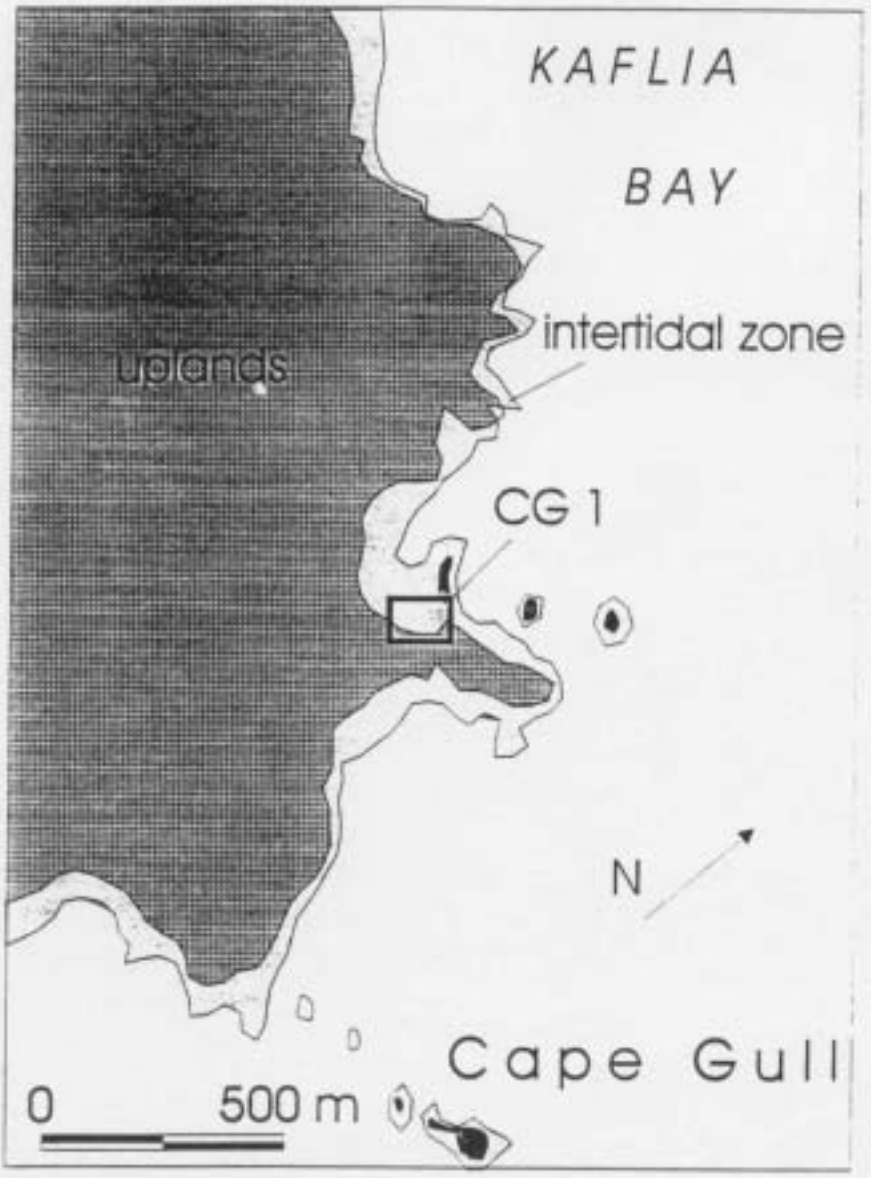

Figure 12. The shoreline between Cape Gull and Kaflia Bay, Shelikof Strait coastline of Katmai National Park and Preserve showing the location of site CG-1. Redrawn from a 1:2000 vertical aerial photograph taken at low spring tide.

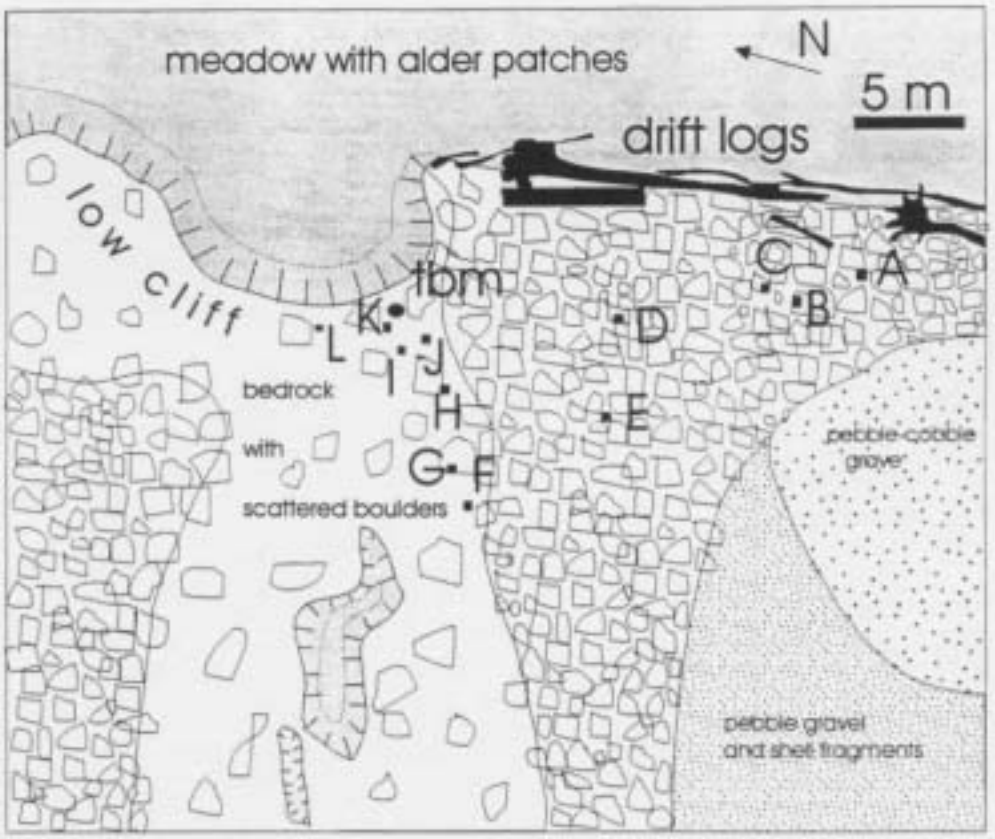

Figure 13. Plan-view sketch map of the Cape Gull study site showing the major substrate types and the approximate locations of the permanent quadrates.

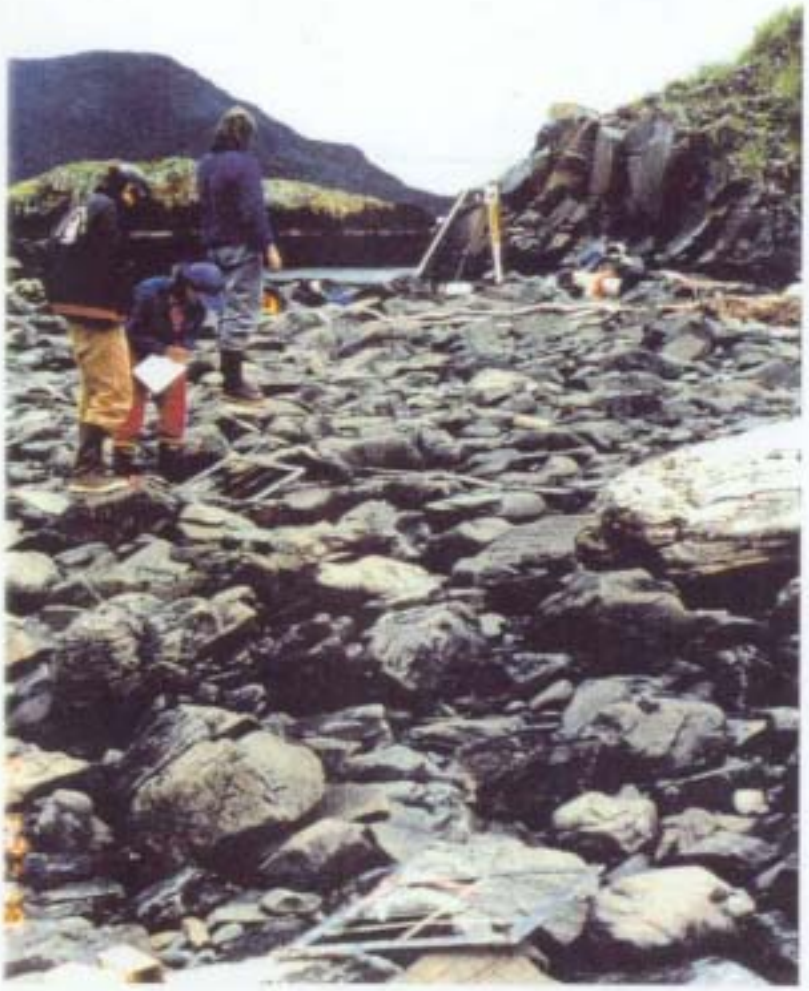

Figure 14. The Cape Gull site (CG-001) in August 1994 looking towards the mouth of Kaflia Bay. The slightly imbricated boulder armor on the upper shore face shelters small patches of remnant surface oiling. Dark lichens cover the sheltered surfaces of most boulders and are indicative of a lengthy time since this boulder armor was last shifted by storm waves.

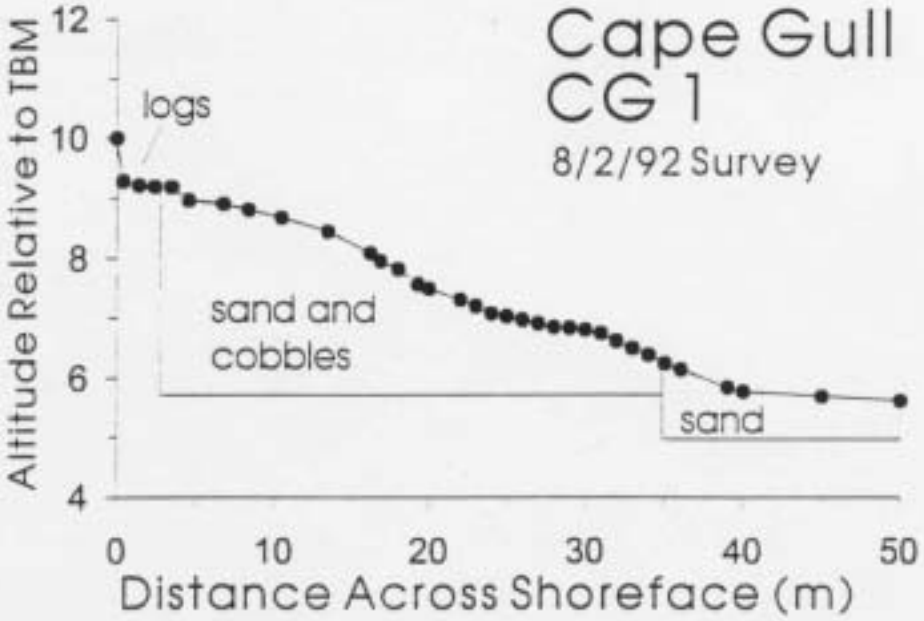

Figure 15. Leveling profile perpendicular to the shore across the Cape Gull study site.

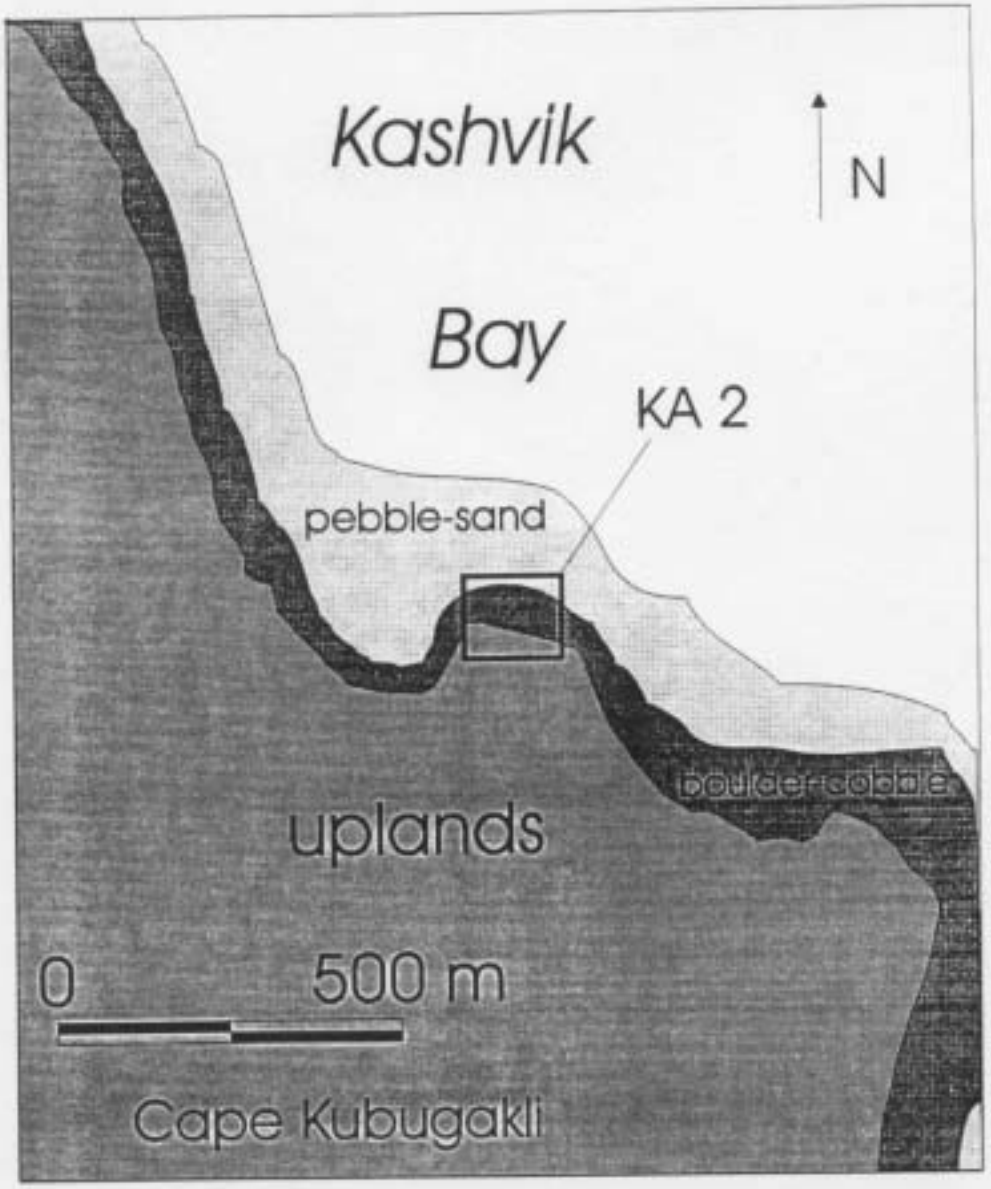

Figure 16. Location of the KA-2 site in outer Kashvik Bay, Shelikof Strait coastline of Katmai National Park and Preserve. Redrawn from a 1:2000 vertical aerial photograph taken at low spring tide.

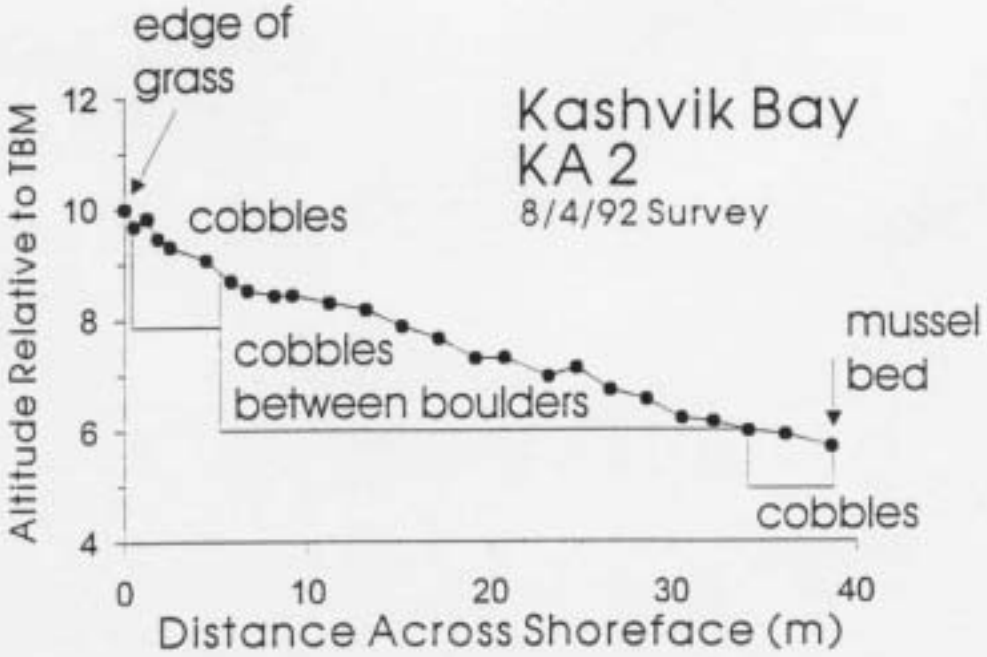

Figure 17. Leveling profile perpendicular to the shore across the Kashvik Bay study site.

Figure 18. The upper shoreface of the Kashvik Bay study site (KA-002) showing the armor of large boulders surrounded by cobbles and small boulders. Since 1992, a layer of cobbes and small boulders has been transported into the site area, filling spaces between large boulders to depths of 20 to 40 cm and burying surface oiling. Shelikof Strait in the distance.

Figure 19. Subsurface oil at the Kashvik Bay study site (KA-002), August 1994. This oil was buried under 20 to 40 cm of cobbles and small boulders by longshore drift occurring sometime between 1992 and 1994. In August of 1994, this site was superficially clean of all oil.

Figure 20. Subsurface oil at the Cape Douglas study site (CD-003A), August 1994. This beach cobble "dip stone" was extracted from the substrate between boulders. Mousse extends to an unknown depth.

APPENDIX B

TABLE OF CONTENTS

APPENDIX B

SUPPLEMENTAL INFORMATION FOR KENAI FJORDS NATIONAL PARK SITE (McArthur Pass)

Introduction

This site was visited in both 1992 and 1994 as part of the oil persistence study. Methods used were the same as for the Katmai National Park study sites (see main body of text). Oil samples were collected in both 1992 and 1994, however, the 1992 samples were lost at the Auke Bay Laboratory prior to analysis, and results of the 1994 samples are reported in Table 2 of the main text. The major differences between this site and the Katmai ones are: 1.) geomorphology, and 2.) distance from the origin of the *Exxon Valdez* oil spill (Figure 1 of main text). A geomorphological description of the Outer Kenai Peninsula follows. It is of interest to note that oil struck parts of the Kenai Fjords coast at about 11 days (Figure 1, main text), which puts the original oiling of that coast as approximately the same age as the 11-day old EVO used in the weathering model and for comparison with all the samples taken in this study.

Geomorphology of the Outer Kenai Coast

Along the Gulf of Alaska flank of the Kenai Mountains, active tectonism and glacial erosion have created an intricate, bedrock coastline. Pleistocene glaciers exploited fault systems and weaker rock types to carve deep fjords between these near-coastal mountains and the outer continental margin. A large percentage of the total shoreline is contained within fjords. Rivers are short, steep, and relatively small; consequently they are unimportant generally as suppliers of sediments to this coastline. The coast of the Kenai Peninsula experiences a wider range of wave energies than does Prince William Sound, Kachemak Bay, or Cook Inlet. Consequently shorelines there show a wider range of geomorphic types than in southern Prince William Sound north of Montague Island. Shoreline terminology follows Michel et al. (1978), Domeracki et al., (1981), and Michel and Hayes (1994).

Exposed bedrock shorelines are abundant in the Kenai Fjords area. They consist of either bedrock cliffs or wave-cut platforms. Bedrock cliffs are often fronted by a narrow (< 10 m wide) beach of locally quarried cobbles and boulders. Local lithology plays an important role in determining beach sediment types. In areas experiencing long-term downwarping, bedrock cliffs often enter directly into the sea. Cliff heights range from several meters to 50+ m. Resistant granitic bedrock has created spectacular cliffs >300 m high in the complex, sunken topography of the Pye and Chiswell Islands, Aialik Peninsula, and Harris Peninsula.

Wave-cut platforms are rare in the Kenai Fjords area although common in Shelikof Strait, Cook Inlet, and southern Prince William Sound. Net Holocene submergence of the Kenai coastline is probably responsible for the rarity of wave-cut platforms there. Typically long intervals of relatively stable sea level are required to cut such platforms into bedrock.

Sheltered bedrock shorelines occur where wave energy is low. They typically have relief varying between 2 and 10 m and are of variable steepness. They are often backed by steep, vegetated slopes. Narrow cobble/boulder beaches less than 10 m wide are common

along sheltered bedrock shorelines. This type of shoreline is relatively rare in the Kenai Fjords though examples occur along the western shore of Nuka Island and in sheltered embayments within the granitic plutons of the Pye Islands, Harris Peninsula, and southern Aialik Peninsula. This type of shoreline grades into rocky rubble slopes in parts of Prince William Sound (Michel and Hayes, 1994).

Pocket beaches are common between bedrock headlands along both sheltered and exposed shorelines. Pocket beaches vary in width from several meters to several hundred meters. On pocket beaches with high wave energy, the predominate sediments are rounded boulders and cobbles. Weathering of the flanking headlands and the backshore provides most of the sediments on pocket beaches. Bedrock joint spacing and wave energy play an important role in determining sediment size and shape. Headlands greatly limit the longshore exchange of sediments between neighboring pocket beaches. Along sheltered shorelines, pocket beaches can contain a wide variety of sediment types ranging from angular boulders to sands and even silts at depth. Commonly, a lag of boulders and cobbles armors finer sands and pebbles at depth on pocket beaches along sheltered shorelines. Relict soils, terrestrial peats, and dead trees commonly outcrop in the intertidal zones of pocket beaches located in areas of long-term downwarping. These downwarped surfaces are as old as 1400 years BP in southern Prince William Sound (Plafker, 1969). Their persistence in the intertidal zone attests to the stability of pocket beach sediments along sheltered shorelines.

Linearly continuous beaches occur in three settings along the Kenai coastline. The first is on bayhead deltas developed in the sheltered waters of fjords where rivers are the predominant sediment source. Beaches of sands, pebbles, and cobbles develop on the delta surface away from active distributary mouths. Shoreface gradients are usually low. Fine sand and silt are widespread in the lower intertidal zone. Glacier advances and retreats may exert important effects over bayhead delta dynamics because many of the streams on the Kenai Peninsula carry glacially-derived sediments. Delta tidal flats exist on sheltered portions of large bayhead delta systems, for instance, in the east arm of Port Dick and in Beauty Bay.

Linearly continuous beaches also occur where glacial outwash trains intersect the coast, a at the Yalik Glacier foreland in Nuka Passage, or the Bear Glacier Foreland in Resurrection Bay, or at the head of Harris Bay on the east side of the entrance of Northwestern Fjord. In this latter case, glacier-outwash issuing from the terminus of the Northwestern Glacier when it reached successive late Holocene maximum positions was reworked into a linearly continuous beach of sand, cobbles, and boulders.

A barrier beach is a berm of unconsolidated, wave-deposited sediment standing seaward of lower-lying subaerial terrain. Barrier beaches can occur in pocket beaches, flanking tidal flats, and along linearly continuous beaches. Barrier beaches are relatively common in the Kenai Fjords area because tectonic subsidence is drowning the coast, causing barrier beaches to move onshore and to dam small lakes, swamps, and lagoons. Good examples of barrier beaches and their enclosed wetlands are in Quicksand Cove (Aialik Bay) and Bulldog Cove (Resurrection Bay).

Spits are a rarity along the Kenai coastline for three reasons: the scarcity of sand and pebble sediments, the interference of rocky headlands with longshore transport, and the youthfulness of most of the shoreline. Spits usually occur in the narrow channels between islands. Tombolos, spits linking the mainland to an island or a spit linking two islands, are more common but are usually small.

Salt marshes also are rare in the Kenai fjords. They usually occur in bedrock-controlled basins and channels along sheltered shorelines. Salt marshes are usually <1 km2 in extent and typically exist as widely dispersed, < 100 m2 patches of marsh. Other fine-grained depositional environments, such as sand beaches and mud-flats also are rare.

Data provided by Hayes (1986) provide a synthesis for the occurrence of different shoreline types along the outer Kenai Peninsula, southern Prince William Sound and the entire shoreline of Montague Island. Rocky headlands comprise about 50% of these shorelines. This category includes both the exposed and sheltered bedrock shorelines described earlier. Beaches, including pocket beaches and linearly-continuous ones, comprise about 32% of the total. Wave-cut platforms comprise about 10% and the remaining 8% is divided between tidal flats and salt marshes.

Tables and Figures Attached

TABLE 1. Oil Cover and Quadrat Arrangement at McArthur Pass Fate and Persistence Monitoring Site, Segment MR-1, 8/23/94

Quadrat	% Oil Cover	Oil Description	Relative Elevations of Marker Bolts (m)	Bearing from Bench Mark (degrees) [b]	Distance from Bench Mark (m)[c]	Distances to Other Bolts (cm)	Quadrat's Long-axis Orientation (degrees)
A	25	coat with small amount of asphalt	2.56	35	8.01	to B = 0.62	270 vertical
B	14	coat with limited interstitial asphalt with embedded fines	2.69	38	7.51	to C = 2.11	166
C	13	coat, limited interstitial mousse	2.43	46	5.73	to D = 0.80	200
D	12	coat, interstitial asphalt with embedded fines	2.41	42	5.07	to E = 1.25	290
E	26	coat, limited interstitial mousse	2.58	54	4.53	to F = 2.62	314
F	13	coat	3.02	79	5.81	to G = 3.50	304 vertical
G	33	coat, asphalt	2.62	83	2.36	to H = 0.83	235
H	17	coat, limited tar	2.71	88	2.96	to I = 0.50	238 [a]
I	11	coat, interstitial tar	2.798	107	3.03	to J = 2.40	316
J	12	interstitial tar with embedded fines, trace of coat	2.45	160	1.86	to K = 7.20	270
K	9	interstitial tar with embedded fines	2.94	155	9.30	to L = 2.33	335
L	12	coat, interstitial tar with embedded fines	2.92	153	11.33	to M = 4.24	252
M	22	interstitial tar with embedded fines	2.87	161	15.06	to N = 6.12	345
N	30	interstitial tar with embedded fines	2.97	167	20.85	to O = 2.98	282
O	13	interstitial tar with embedded fines	2.81	170	23.64	to P = 6.80	350 [a]
P	12	interstitial tar with embedded fines	3.44	165	30.10	to Q = 4.80	8
Q	15	coat, interstitial tar with embedded fines	3.29	170	33.96	to TBM - MR-1 = 2.3	28

[a] Stadia rod is set on top of bolt. These altitudes are relative to one another.

[b] relative to magnetic north. While internally consistent, all these bearings may be about 6 degrees off of magnetic north due to disturbance of the setup by a passerby.

TABLE 2. Subsurface Oiling Described under Randomly Selected "Dip-Stones" at McArthur Pass, Segment MR-1

Stone Number	Location	Description of Oiling
1	near quadrat M	2 stones clean, 1 stone clean to 1.5 cm depth then 1 cm of tar and 1 cm of mousse
2	40 cm southwest of quadrat L	tar ring stone to 1 cm below surface
3	1 m southeast of quadrat L	tar mixed with fines extends to depth of 2 cm
4	30 cm north of quadrat N	tar extends to depth of 2 cm
5	1 m east of putty dot #3*	mousse extends to 2 cm depth
6	20 cm south of quadrat O	tar extends to 2 cm depth, clean below

* a marker from another National Park Service study at the same site

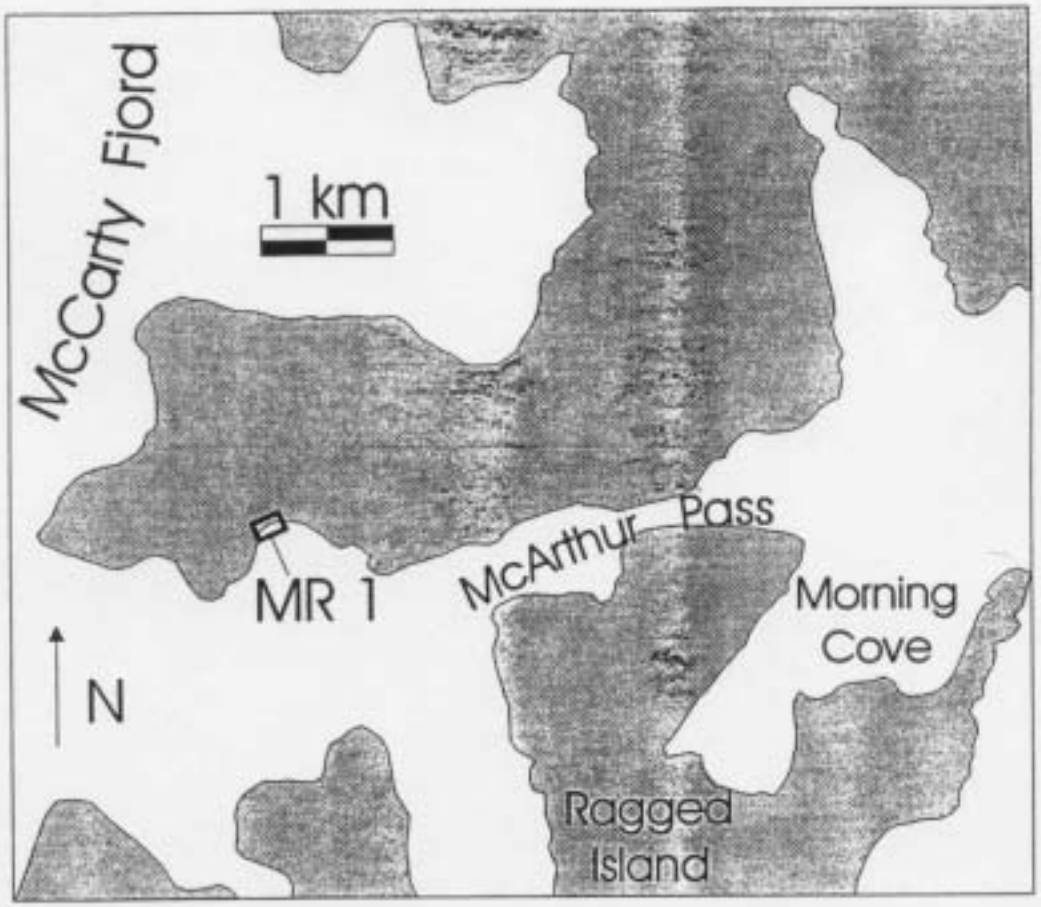

Figure 1. Location of the MR-1 site on the northern shore of McArthur Pass, southeastern coast of the Kenai Peninsula in the Kenai Fjords National Park and Preserve.

Figure 2. A portion of the McArthur Pass (MR-1) site in August 1994. Bedrock crops out in the right foreground. Conifer trees along the edge of the supratidal zone were killed by salt water inundation after the 1964 earthquake, which caused one to two meters of subsidence in this part of Kenai Fjords National Park.

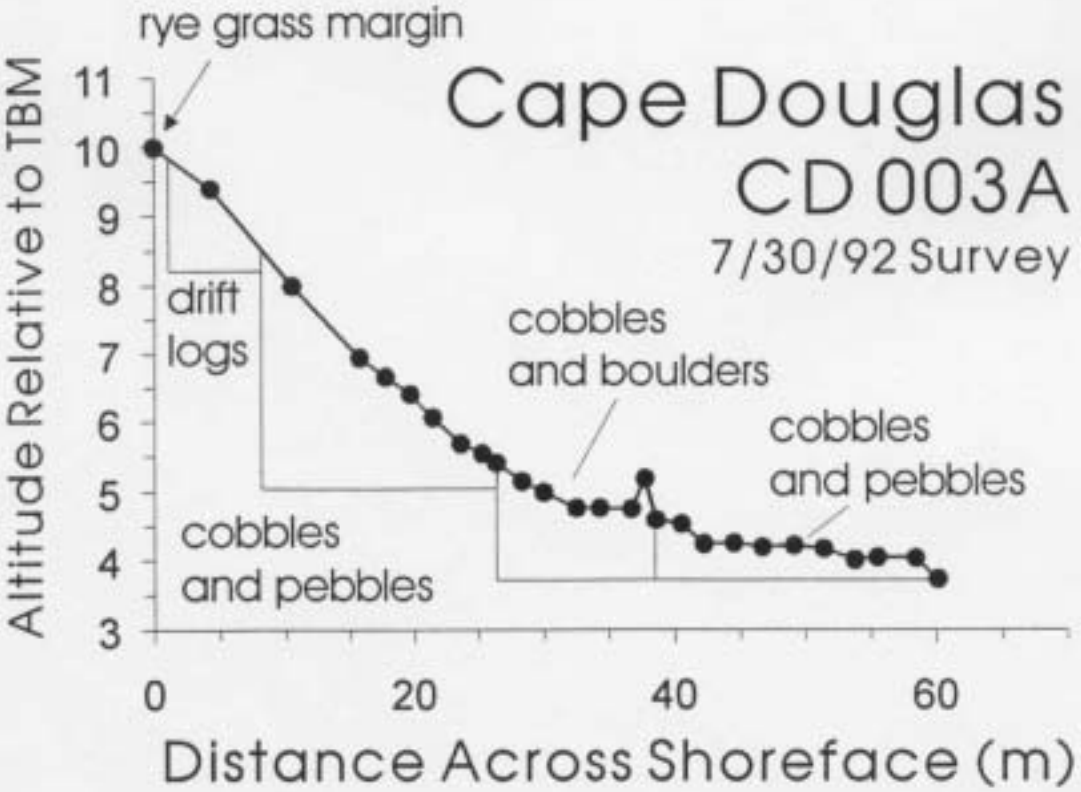

Figure 3. Leveling transect perpendicular to the shore showing the beach profile at the Cape Douglas study site.

APPENDIX C

HYDROCARBON DATABASE

APPENDIX C

HYDROCARBON DATABASE

This table presents the hydrocarbon data for all 25 oiled sediment samples analyzed by gas chromatography/mass spectroscopy (GC/MS). Data for both aromatic and alkane hydrocarbons are presented on a dry weight basis. Site abbreviations represent: CDOUG= Cape Douglas, CGULL= Cape Gull, KIUKP= Kiukpalik, KASHB=Kashvik Bay, KUBUG= Kubugakli, NINAI= Ninagiak, MCARP= McArthur Pass. **Note**: Numbers in italicized bold are below the method detection limit (MDL) adjusted for sample size (mass).

Sample ID #	ID	302708	302709	302714	302715	304902	500204	500205
Date Collected	Datecol	7/30/92	7/31/92	8/2/92	8/2/92	10/12/92	8/6/94	8/6/94
Location	Locatabv	CDOUG	CDOUG	CGULL	CGULL	CGULL	CDOUG	CDOUG
Wet Weight	Wetwt	0.027	0.014	0.041	0.02	0.001	0.02	0.017
Dry Weight	Drywt	0.025	0.013	0.037	0.018	0.001	0.02	0.017
Naphthalene	Naph	***0***	***0***	***0***	***0***	***0***	578.01	***254.75***
2-Methyl-Naphthalene	Menap2	**0**	***496.08***	***0***	***0***	10137.33	6507.43	4235.5
1-Methyl-Naphthalene	Menap1	***147.3***	844.3	***0***	***0***	12928.61	7014.85	5329.82
2,6-Dimethyl-Naphthalene	Dimeth	2378.59	6441.08	***0***	***0***	49635.38	29182.92	27880.13
C2-Naphthalenes	C2naph	14082.11	33452.93	***0***	***0***	241185.42	140387.9	139727.1
2,3,5-Trimethyl-Naphthalene	Trimeth	9558.65	17987.31	792.34	***0***	87143.57	93368.4	93564.35
C3-Naphthalenes	C3naph	47897.02	97995.21	4869.05	2397.51	482719.43	448771.8	458512.34
C4-Naphthalenes	C4naph	29123.51	49936.07	19222.67	18162.54	196480.42	367499.18	363646.33
Biphenyl	Biphenyl	***103.58***	***334.93***	***0***	***0***	***2631.8***	3449.63	2555.83
Acenaphthylene	Acenthy	***0***	***0***	***0***	***0***	***0***	***0***	***0***
Acenaphthene	Acenthe	***0***	***0***	***0***	***0***	***0***	***1244.44***	***1448.86***
Fluorene	Fluroene	1529.8	2725.67	***0***	***0***	***12430.67***	18804.91	17268.21
C1-Fluorenes	C1fluor	8549.22	13983.8	1194.12	***1206.44***	53387.49	116418.9	104367.51
C2-Fluorenes	C2fluro	29917.32	45460.04	16020.7	18798.04	166398.6	236974.29	213531.71
C3-Fluorenes	C3fluro	22575.66	31875.32	17668.66	20285.18	106338.9	67953.42	58587.53
Dibenzothiophene	Dithio	7936.36	13826.72	***152.1***	***197.17***	56571.86	59543.28	61446.56
C1-Dibenzothiophenes	C1dithio	24610.32	38133.23	1409.15	***832.63***	139233.21	121606	121206.51
C2-Dibenzothiophenes	C2dithio	48695.3	75370.58	28983.23	35743.68	245650.51	141041.79	137506.21
C3-Dibenzothiophenes	C3dithio	53953	82293.79	45230.44	55064.88	242147.71	164768.9	156384.31
Phenanthrene	Phenanth	9124.88	15727.34	***0***	***0***	35999	99461.79	100561.9
1-Methyl-Phenanthrene	Mephen1	15422.99	24806.85	417.62	***238.33***	88285.43	77156.97	73556.08
C1-Phenanthrenes	C1phenan	43012.97	67334.5	1172.5	***319.99***	218786.42	321161.81	304922.83

C2-Phenanthrenes	C2phenan	86194	131901.32	44117.44	42413.21	410383.83	439539.8	421053.02
C3-Phenanthrenes	C3phenan	71246.89	108366.15	59178.35	69399.13	338365.61	370730.4	350497.02
C4-Phenanthrenes	C4phenan	20998.28	31738.24	18397.83	19026.1	84299.32	100626	101993.51
Anthracene	Anthra	***939.84***	***1509.85***	***156.34***	***195.17***	***7708.04***	5680.17	6353.19
Fluoranthene	Fluroant	923.54	1407.89	550.24	532.61	4601.25	1580.93	1391.38
Pyrene	Pyrene	1343.44	***2020.02***	1048.07	***1241.56***	***6243.02***	9354.32	8704.19
C1-Fluoranthenes	C1fluora	5738.09	8444.81	4733.18	5189.02	18860	40095.44	39007.48
Benzo-a-anthracene	Benanth	***298.29***	***537.88***	***271.19***	***446.88***	***2282.16***	3264.81	3824.37
Chrysene	Chrysene	6406.86	9054.4	4561.28	5926.86	27554.3	40526.14	42618.02
C1-Chrysenes	C1chrys	7536.87	10548.14	6345.33	8458.03	19016.06	66165.09	71243.75
C2-Chrysenes	C2chrys	5408.67	8000.58	5230.81	7173.64	21792.44	51570.67	55812.86
C3-Chrysenes	C3chrys	4647.11	6942.76	4292.6	5754.27	11712.38	36425.12	46573.32
C4-Chrysenes	C4chrys	***200.56***	***263.03***	304.23	397.67	***0***	7870.8	9336.86
Benzo-b-fluoranthene	Benzobfl	1061.16	1609.06	788.11	1130.49	***6519.85***	5240.44	5231.64
Benzo-k-fluoranthene	Benzokfl	0	0	0	0	0	0	0
Benzo-e-pyrene	Benepy	1617.45	3235.39	1387.03	2302.98	***16795.93***	10129.84	10389.83
Benzo-a-pyrene	Benapy	***408.55***	***0***	***247.39***	***0***	***0***	1360.99	1458.56
Perylene	Perylene	***178.1***	***0***	***0***	***0***	***0***	***556.38***	***523.19***
Indeno(1,2,3-c,d)pyrene	Indeno	***0***	***0***	***0***	***0***	***0***	***0***	***436.03***
Dibenzoanthracene	Dibenz	***0***	***0***	***49.55***	***0***	***0***	***792.27***	***730.49***
Benzoperylene	Benzop	253.08	314.57	205.13	309.57	***0***	2251.19	1110.79
n-Decane	C10alk	***0***	***0***	***0***	***0***	***0***	***0***	***0***
n-Undecane	C11alk	***0***	***0***	***0***	***0***	***0***	***1117.5***	***959.9***
n-Dodecane	C12alk	***645.84***	***1674.62***	***0***	***0***	***19801***	9341.6	5259.4
n-Tridecane	C13alk	6994.08	17721.85	***0***	***0***	167372.01	81026.7	56879.5
n-Tetradecane	C14alk	23151.96	50790.92	***0***	***0***	302515.01	452382.18	337988.83
n-Pentadecane	C15alk	76751.28	153128.77	4095.57	***0***	715657.03	1183129.97	985580.05
n-Hexadecane	C16alk	112517.64	222913.39	5100.62	***0***	1020930.05	1670249.96	1408610.08
n-Heptadecane	C17alk	150236.64	304572.16	13941.11	***806.67***	1301350.06	2225129.95	1910370.1
Pristane	Pristane	164657.88	280120.62	109687.19	119618.89	1135450.05	1960469.96	2022160.11

n-Octadecane	C18alk	140357.88	278768.01	10472.73	3301.11	1184440.06	2039519.95	1861670.1
Phytane	Phytane	111217.32	172408.93	71261.33	88806.66	637507.03	1373189.97	1398650.08
Nonadecane	C19alk	132844.32	266081.85	7760.08	2174.44	1142230.05	1613809.96	1545110.08
n-Eiosane	C20alk	146976.12	285275.85	19005.16	10222.22	1216370.06	2067209.95	2018900.11
n-Heneicosane	C21alk	130746.96	253940.62	13671.84	5203.33	1131300.05	1855749.96	1843670.1
n-Docosane	C22alk	132241.68	249253.85	15814.92	10393.33	1027890.05	1310619.97	1316390.07
n-Tricosane	C23alk	113007.96	220371.85	8050.41	*0*	881741.04	1170489.97	1213000.07
n-Tetracosane	C24alk	117148.68	222910.16	19115.97	*0*	864223.04	1268549.97	1338970.07
n-Pentacosane	C25alk	106754.76	193006.16	20853.49	7981.11	723341.03	1180429.97	1260970.07
n-Hexacosane	C26alk	104419.8	179830.01	31349.49	3384.44	667343.03	1127309.97	1223540.07
n-Heptacosane	C27alk	97198.92	159400.77	33981.24	*0*	581490.03	844371.29	9367.4
n-Octacosane	C28alk	65599.2	106937.39	14176.03	*0*	311915.01	611847.49	651499.41
n-Nonacosane	C29alk	64215.72	97360.31	18996.3	6921.11	309529.01	548390.61	600019.72
n-Triacontane	C30alk	61408.8	93330.46	28274.49	16472.22	315551.01	480778.18	505655.62
n-Dotriacontane	C32alk	41109.12	60526.31	24375.05	22468.89	237836.01	331364.09	364016.21
n-Tetratriacontane	C34alk	51271.92	70589.08	32177.24	54581.11	275066.01	385848.09	371145.93
Unresolved Complex Mix	UCM	16686000.43	24338462.29	15014865.28	19877777.33	89320004.24	201999995.48	207700011.29

Sample ID#	ID	500213	500214	302710	302711	302716	302717	304901
Date Collected	Datecol	8/10/94	8/10/94	7/3/92	7/3/92	8/4/92	8/4/92	9/29/92
Location	Locatabv	CGULL	CGULL	KIUKP	KIUKP	KASHB	KASHB	KUBUG
WetWeight	Wetwt	0.122	0.203	0.014	0.001	0.02	0.002	0.002
Dry Weight	Drywt	0.122	0.203	0.012	0.001	0.018	0.001	0.002
Napththalene	Naph	0	9.32	0	0	112.24	0	0
2-Methyl-Naphthalene	Menap2	13.23	12.77	6790.61	7466.71	1244.39	50806.06	2171.89
1-Methyl-Naphthalene	Menap1	25.87	5.31	7156.15	10663.06	1599.06	53214.12	5611.32
2,6-Dimethyl-Naphthalene	Dimeth	1235.05	25.48	24588.59	47598.92	7673.06	170042.65	42089.39
C2-Naphthalenes	C2naph	6121.51	353.41	114029.26	231078.6	36180.48	782599.66	200183.51
2,3,5-Trimethyl-Naphthalene	Trimeth	6475.59	715.83	37938.16	79968.66	16268.13	238269.61	77021.5
C3-Naphthalenes	C3naph	33573.89	5525.71	217023.23	446043.52	91254.77	1360007.44	436203.11
C4-Naphthalenes	C4naph	33789.21	29448.91	90286.03	175845.1	42642.31	524408.65	206161.71
Biphenyl	Biphenyl	128.59	25.05	2818.62	1578.83	499.5	17306.56	587.84
Acenaphthylene	Acenthy	0	0	0	0	0	0	0
Acenaphthene	Acenthe	130.43	45.09	0	0	5.96	0	0
Fluorene	Fluroene	322.03	39.12	5133.04	10094.37	1431.24	32099.52	9552.39
C1-Fluorenes	C1fluor	7160.68	2770.39	26851.41	46684.38	11698.9	154853.79	9999.43
C2-Fluorenes	C2fluro	18739.65	18504.04	75127.78	147506.41	34746.88	420539.61	108155.21
C3-Fluorenes	C3fluro	10591.9	14742.07	54180.86	95811.94	24250.13	260170.81	60513.03
Dibenzothiophene	Dithio	1161.67	101.82	20836.55	45739.62	6715.22	131668.91	36753.37
C1-Dibenzothiophenes	C1dithio	10315.76	2771.02	52774.41	115511.01	22837.62	286124.61	26497.73
C2-Dibenzothiophenes	C2dithio	21339.21	21704.76	100132.2	208108.42	49668.08	534662.03	95847.01
C3-Dibenzothiophenes	C3dithio	25534.75	41523.02	109946.38	218328.81	54906.07	571496.22	80031.69
Phenanthrene	Phenanth	2235.85	223.49	26056.49	15563.27	7032.57	109215.87	104366.11
1-Methyl-Phenanthrene	Mephen1	6142.28	1233.88	32861.21	76798.93	14782.27	181978.63	90476.78
C1-Phenanthrenes	C1phenan	25076.8	5164.02	92283.2	188011.91	40026.74	488297.62	373013.33

C2-Phenanthrenes	C2phenan	53533.76	54372.33	176521.92	342900.7	83728.26	905835.04	474740.43
C3-Phenanthrenes	C3phenan	48408	85705.71	145327.82	288379.83	71606.86	741400.04	331084.2
C4-Phenanthrenes	C4phenan	13111.78	27630.97	42985.66	75338.75	19870.32	185541.74	80119.39
Anthracene	Anthra	510.4	592.71	2015.88	6125.43	833.68	15271.76	7663.99
Fluoranthene	Fluroant	151.59	207.77	1907.28	4152.74	857.71	9968.14	6025.73
Pyrene	Pyrene	1166.11	2199	2790.06	5583.17	1359.93	14444.48	8882.98
C1-Fluoranthenes	C1fluora	5061.72	10969.43	11450.16	14941.63	5872.48	51173.94	25872.95
Benzo-a-anthracene	Benanth	95.96	130.81	759.27	2840.26	422.52	6191.1	2127.62
Chryssene	Chrysene	3810.18	5609.72	12310.94	29843.1	6512.67	69772.75	34148.99
C1-Chrysenes	C1chrys	6508.33	9569.94	15307.96	18166.32	7807.93	65602.3	41233.67
C2-Chrysenes	C2chrys	5027.83	8698.12	12144.91	20219.04	6356.6	61027.66	34385.26
C3-Chrysenes	C3chrys	4612.25	9115.42	10001.99	13314.02	5161.6	53939.9	13206.64
C4-Chrysenes	C4chrys	907.07	2006.96	632.15	456.2	238.64	1654.7	0
Benzo-b-fluoranthene	Benzobfl	475.03	824.62	2507.14	5108.56	1037.97	11747.76	6059.17
Benzo-k-fluoranthene	Benzokfl	0	0	0	0	0	0	0
Benzo-e-pyrene	Benepy	945.66	1811.54	5197.43	6989.75	2312.2	26391.04	9577.11
Benzo-a-pyrene	Benapy	119.42	226.51	0	0	0	0	0
Perylene	Perylene	66.82	112.43	0	0	0	0	0
Indeno(1,2,3-c,d)pyrene	Indeno	0	107.97	0	0	0	0	0
Dibenzoanthracene	Dibenz	51.92	201.69	0	0	0	0	0
Benzoperylene	Benzop	200.36	572.82	231.41	0	152.83	2316.74	0
n-Decane	C10alk	0	0	0	0	0	0	0
n-Undecane	C11alk	0	0	1680	0	1038.89	0	0
n-Dodecane	C12alk	611.87	0	14891.33	28293	4376.67	120642.01	21940
n-Tridecane	C13alk	4616.79	0	75730.67	161071.01	21587.78	586042.03	132211.01
n-Tetradecane	C14alk	10520.09	140.5	147050.17	323467.02	42928.89	1016314.05	331497.02
n-Pentadecane	C15alk	24717.87	1906.9	313541.68	656005.03	98765.55	1973588.09	439701.02
n-Hexadecane	C16alk	29332.12	3957.2	375413.51	829255.04	117642.22	2359920.11	1099690.05
n-Heptadecane	C17alk	39894.02	3215.7	471517.68	1028320.05	152313.33	2968480.14	1374460.07
Pristane	Pristane	107209	48749	473085.68	1061680.05	213672.22	2671700.13	1202750.06

n-Octadecane	C18alk	35476.25	1075.8	428578.51	989515.05	137417.77	2689820.13	1321750.06
Phytane	Phytane	73490.44	23848.4	258127.34	595553.03	119615.55	1461852.07	710022.03
Nonadecane	C19alk	24199.15	1018.2	407092.01	977243.05	130351.11	2528720.12	1168780.06
n-Eiosane	C20alk	36727.98	3301.1	432267.51	1046680.05	147057.77	2684740.13	1286390.06
n-Heneicosane	C21alk	37578.79	2387.9	388531.51	926826.04	133301.11	2423860.12	1140390.05
n-Docosane	C22alk	36955.91	3642.5	371682.51	897452.04	133514.44	2260020.11	1187220.06
n-Tricosane	C23alk	31873.11	1461.3	331312.34	772683.04	117867.78	1972650.09	1013230.05
n-Tetracosane	C24alk	41256.93	10528.9	337944.84	761375.04	129752.22	1962028.09	972580.05
n-Pentacosane	C25alk	42341.01	9145.1	297679.68	632940.03	118898.89	1650374.08	799786.04
n-Hexacosane	C26alk	42867.8	2635.6	272984.84	579193.03	119840	1505824.07	640777.03
n-Heptacosane	C27alk	321.13	14705.6	252313.84	509261.02	110214.44	1366486.06	499090.02
n-Octacosane	C28alk	30732.46	4351.2	168892.51	399581.02	70597.78	783006.04	433174.02
n-Nonacosane	C29alk	34822.31	10801.4	161150.5	270547.01	68406.67	744906.04	361624.02
n-Triacontane	C30alk	32911.31	18845.1	148888.84	289959.01	65638.89	725594.03	313021.01
n-Dotriacontane	C32alk	25480.52	21852.8	101203.67	233847.01	47597.78	507686.02	303510.01
n-Tetratriacontane	C34alk	35590.59	37393.4	112075.84	256825.01	51506.67	613236.03	246628.01
Unresolved Complex Mix	UCM	12610000.14	14169999.59	35233334.42	83200003.95	18544444.03	223600010.62	64120003.1

Sample ID #	ID	500207	500208	500216	500217	302713	302712	304903
Date Collected	Datecol	8/8/94	8/8/94	8/11/94	8/11/94	8/1/92	8/1/92	12/10/89
Location	Locatabv	KIUKP	KIUKP	KASHB	KASHB	NINAI	NINAI	NINAI
WetWeight	Wetwt	0.025	0.03	0.024	0.021	0.001	0.01	0.002
Dry Weight	Drywt	0.025	0.03	0.024	0.021	0.001	0.009	0.002
Naphthalene	Naph	***0***	***139.96***	897.72	638.77	***0***	***0***	***0***
2-Methyl-Naphthalene	Menap2	5846.43	8518.03	12607.11	2273.13	***0***	***162.91***	4692.83
1-Methyl-Naphthalene	Menap1	6440.38	9260.28	13237.74	2628.26	***1472.66***	***732.31***	8627.07
2,6-Dimethyl-Naphthalene	Dimeth	36893.05	32970.39	40299.43	13833.9	***21763.74***	9048.91	46601.37
C2-Naphthalenes	C2naph	164273.6	148455.2	184513.2	62718.18	120678.4	47926.4	222147.81
2,3,5-Trimethyl-Naphthalene	Trimeth	79251.46	63237.76	68565.39	37811.54	54879.9	24149.89	81134.93
C3-Naphthalenes	C3naph	418078.91	325759.81	368986.19	184830.9	301225.7	134428.1	468024.02
C4-Naphthalenes	C4naph	331241.69	279293.59	261852.3	153359.09	133107.71	71049.15	234008.01
Biphenyl	Biphenyl	3130.61	3897.96	4931.28	1320.3	***0***	***309.83***	***1273.89***
Acenaphthylene	Acenthy	***0***	***0***	***0***	***0***	***0***	***0***	***0***
Acenaphthene	Acenthe	***1464.67***	***1040.7***	***1464.65***	***604.47***	***0***	***0***	***0***
Fluorene	Fluroene	10219.4	9848.26	12725.03	5186.06	***5078.66***	***2201.22***	***8800.74***
C1-Fluorenes	C1fluor	76509.55	65325.53	62119.22	38375.43	41313.69	18736.55	***11418.33***
C2-Fluorenes	C2fluro	165682.71	153582.7	125091.2	87155.51	119882.61	62180.36	112929.71
C3-Fluorenes	C3fluro	69246.15	59695.7	65208.02	45660.19	82423.96	47119.48	68388.96
Dibenzothiophene	Dithio	32654.4	30468.07	37022.44	13710.3	32177.02	12741.68	43885.4
C1-Dibenzothiophenes	C1dithio	73148.43	118303.1	80250.8	46402.31	95015.87	48179.7	41373.47
C2-Dibenzothiophenes	C2dithio	109072.1	134357.7	139007.3	89333.53	183549.1	101979.09	149400.8
C3-Dibenzothiophenes	C3dithio	129744.6	166239.59	160802.6	107162.1	197396.1	117710	128633.01
Phenanthrene	Phenanth	59959.02	55835.37	60919.8	26081.9	8028.86	12869.87	82760.69
1-Methyl-Phenanthrene	Mephen1	60576.29	78313.21	83251.55	46276.72	62526.43	27883.57	83427.33
C1-Phenanthrenes	C1phenan	249933	244840.59	346153.19	190179.4	151677.01	78560.48	324112.42

C2-Phenanthrenes	C2phenan	346055.6	345797.68	479163.5	302167.68	305492.2	173865.66	461644.71
C3-Phenanthrenes	C3phenan	290122.1	286664.81	400374.5	266298.59	265026.33	155735.45	343020.11
C4-Phenanthrenes	C4phenan	88292.66	93030.4	106664.8	72618.74	68753.12	47486.18	87254.64
Anthracene	Anthra	5785.04	3820.1	3733.94	2209.36	*0*	*1568.96*	*8544.7*
Fluoranthene	Fluroant	1272.39	1005.67	1877.87	1199.72	*3615.19*	1846.96	6001.4
Pyrene	Pyrene	7067.07	6299.65	9196.84	6075.49	*4991.17*	*2836.54*	*9326.27*
C1-Fluoranthenes	C1fluora	32574.57	28192.02	41341.26	27287.28	13686.93	12701.26	25979.97
Benzo-a-anthracene	Benanth	989.87	1619.4	781.39	*455.05*	*2345.24*	*714.53*	*2783.31*
Chrysene	Chrysene	27348.79	28059.56	18525.83	12568.99	24441.88	13255.22	34678.03
C1-Chrysenes	C1chrys	45855.83	53588.3	30780	20350.83	15943.5	16633.58	38583.73
C2-Chrysenes	C2chrys	35671.83	27737.77	25052.6	16471.5	17247.04	13045.39	33953.18
C3-Chrysenes	C3chrys	30528.1	33585.17	23134.4	16775.91	6730.16	11240.73	17823.62
C4-Chrysenes	C4chrys	6033.99	8371.85	4430.66	2635.7	*419.98*	673.54	*179.96*
Benzo-b-fluoranthene	Benzobfl	3397.16	3273.69	2375.16	1583.45	3549.79	2327.28	*4580.97*
Benzo-k-fluoranthene	Benzokfl	*0*	*0*	*0*	*0*	*0*	*0*	*0*
Benzo-e-pyrene	Benepy	6795.8	6630.77	4693.83	3112.51	*5701.97*	5071.94	*10082.82*
Benzo-a-pyrene	Benapy	959.06	866.93	671.52	*429.38*	*0*	*0*	*0*
Perylene	Perylene	*449.24*	*455.37*	*225.38*	*0*	*0*	*0*	*0*
Indeno(1,2,3-c,d)pyrene	Indeno	*0*	*395.97*	*0*	*0*	*0*	*0*	*0*
Dibenzoanthracene	Dibenz	*516.72*	*743.1*	*171.47*	*264.38*	*0*	*0*	*0*
Benzoperylene	Benzop	1548.41	1765.66	1159.45	795.59	*0*	*223.84*	*0*
n-Decane	C10alk	*0*	*0*	*0*	*0*	*0*	*0*	*0*
n-Undecane	C11alk	*1735.5*	*1691.3*	2210.7	*890.7*	*0*	*0*	*0*
n-Dodecane	C12alk	21664.8	18526.8	22597.3	7332.9	*0*	*4343.33*	28364
n-Tridecane	C13alk	129603.5	102069.9	111062.1	42205.5	73786	30613.33	169774.01
n-Tetradecane	C14alk	423008.01	407218.3	419012.82	87914	122643.01	65620	331836.02
n-Pentadecane	C15alk	881610.89	768653.67	764703.63	205056.79	312679.01	164708.89	305464.01
n-Hexadecane	C16alk	1090940.02	921067.67	908442.63	233057.9	432075.02	199987.77	778073.04
n-Heptadeane	C17alk	1401300.02	1160959.97	1103500.01	294557.9	590458.03	257064.44	930428.04
Pristane	Pristane	1582550.02	1411029.97	1176330.01	416697.68	870933.04	346957.77	1081870.05

n-Octadecane	C18alk	1349830.02	982781.35	957750.51	295603.59	569757.03	248518.88	862016.04
Phytane	Phytane	1009250.02	822000.98	765868.63	289363.81	512903.02	225298.88	660572.03
Nonadecane	C19alk	1100630.02	754212.98	765044.38	260265.9	550631.03	235698.88	743587.04
n-Eiosane	C20alk	1432610.02	1036679.98	1033570.01	326048.31	638668.03	271458.88	852456.04
n-Heneicosane	C21alk	1337470.02	940956.17	953625.13	303397.4	599781.03	245135.55	758187.04
n-Docosane	C22alk	943257.39	460202.8	501331.5	272295.81	579389.03	253036.66	806010.04
n-Tricosane	C23alk	884015.14	419050.49	458603.1	256557.2	513599.02	221592.22	689886.03
n-Tetracosane	C24alk	958751.2	468864.58	501006.32	298048.81	538520.03	242198.88	720224.03
n-Pentacosane	C25alk	900760.39	452022.8	478320.5	288583.68	466074.02	224622.22	620972.03
n-Hexacosane	C26alk	870620.51	429977.58	458780.91	294563.09	465088.02	236167.77	569663.03
n-Heptacosane	C27alk	15738.2	343245.18	352779.19	3099.1	426644.02	207552.22	417175.02
n-Octacosane	C28alk	469035.32	406024.49	330638.1	186564.29	234378.01	132268.89	365140.02
n-Nonacosane	C29alk	446221.91	388327.9	321107.19	183134.5	226229.01	133958.89	310257.01
n-Triacontane	C30alk	399154.69	343765.31	306665.1	168426.5	242582.01	131725.55	276459.01
n-Dotriacontane	C32alk	274245.1	256057.09	171054.6	125942.3	185690.01	91803.33	208617.01
n-Tetratriacontane	C34alk	336662.1	291502.09	210022.1	153174.79	225047.01	102922.22	284338.01
Unresolved Complex Mix	UCM	151200002.25	119999997.32	115900001.01	55689999.25	72350003.44	38233332.48	67760003.22

Sample ID #	ID	500201	500202	500210	500211
Date Collected	Datecol	5/27/94	5/27/94	8/9/94	8/9/94
Location	Locatabv	MCARP	MCARP	NINAI	NINAI
WetWeight	Wetwt	0.46	0.022	0.031	0.024
Dry Weight	Drywt	0.39	0.022	0.031	0.024
Naphthalene	Naph	***0***	***111.11***	350.9	429.09
2-Methyl-Naphthalene	Menap2	46.55	3464.17	4813.79	2935.23
1-Methyl-Naphthalene	Menap1	136.91	4110.59	6014.99	3674.94
2,6-Dimethyl-Naphthalene	Dimeth	1388.73	23138.2	20337.25	25138.38
C2-Naphthalenes	C2naph	8701.93	106017.8	96643.23	110199.5
2,3,5-Trimethyl-Naphthalene	Trimeth	10017.09	61502.63	50609.22	57605.62
C3-Naphthalenes	C3naph	48531.62	301816	236103.79	293772.41
C4-Naphthalenes	C4naph	61561.88	234766.9	201619.59	217102.5
Biphenyl	Biphenyl	63.8	2577.55	2450.26	1554.44
Acenaphthylene	Acenthy	***0***	***0***	***0***	***0***
Acenaphthene	Acenthe	***92.01***	***1091.58***	***839.5***	***1021.22***
Fluorene	Fluroene	1112.22	9136.47	8675.63	8505.37
C1-Fluorenes	C1fluor	13046.71	64606.31	62458.51	54515.5
C2-Fluorenes	C2fluro	40763.23	133257.59	146165.79	115728.2
C3-Fluorenes	C3fluro	17378.03	35993.34	63296.37	53865.2
Dibenzothiophene	Dithio	4194.37	34732.65	19352.06	23120.08
C1-Dibenzothiophenes	C1dithio	26402.43	70779.52	80671.7	60762.27
C2-Dibenzothiophenes	C2dithio	33775.29	73225.44	104631.4	107627
C3-Dibenzothiophenes	C3dithio	40709.05	82658.19	129609.2	127198.2
Phenanthrene	Phenanth	7376.62	59852.78	37957.62	43100.4

1-Methyl-Phenanthrene	Mephen1	12740.04	38152.78	57647.33	59184.89
C1-Phenanthrenes	C1phenan	53660.46	156046	179679.79	245149.5
C2-Phenanthrenes	C2phenan	89056.5	205076.7	266107.81	361483.6
C3-Phenanthrenes	C3phenan	72195.44	156985	240243.5	310481.5
C4-Phenanthrenes	C4phenan	24705.01	47855.73	78193.9	83862.5
Anthracene	Anthra	683.94	3827.72	2608.71	2923.95
Fluoranthene	Fluroant	255.21	829.54	787.07	1359.26
Pyrene	Pyrene	1765.01	4524.35	5120.7	7164.06
C1-Fluoranthenes	C1fluora	6953.69	18424.91	25577.21	32007.12
Benzo-a-anthracene	Benanth	741.87	1358.62	1633.44	1598.14
Chrysene	Chrysene	9120.61	35349.71	19606.37	16912.4
C1-Chrysenes	C1chrys	16311.02	53943.1	37618.8	27697.07
C2-Chrysenes	C2chrys	7568.85	40145.56	19768.63	22056.1
C3-Chrysenes	C3chrys	10010.76	25189.22	24449.96	19521.82
C4-Chrysenes	C4chrys	3415.11	7814.42	5919.87	4676.65
Benzo-b-fluoranthene	Benzobfl	1105.84	4370.71	2313.84	2179.46
Benzo-k-fluoranthene	Benzokfl	*0*	*0*	*0*	*0*
Benzo-e-pyrene	Benepy	2244.74	7981.2	4869	4204.82
Benzo-a-pyrene	Benapy	275.72	1374.75	623.92	617.43
Perylene	Perylene	117.22	*1026.23*	*271.6*	*0*
Indeno(1,2,3-c,d)pyrene	Indeno	111.25	*682.49*	*95.94*	*158.54*
Dibenzoanthracene	Dibenz	260.18	*907.2*	*463.83*	*330.57*
Benzoperylene	Benzop	652.74	1047.68	1230.3	1009.9
n-Decane	C10alk	*68.48*	*0*	*0*	*0*
n-Undecane	C11alk	56.19	997.8	1452.7	889.2
n-Dodecane	C12alk	180.54	6446.9	14795.3	7975.3
n-Tridecane	C13alk	934.32	48075.4	83709.8	56908.3

n-Tetradecane	C14alk	3585.83	231511.2	247549.59	218491
n-Pentadecane	C15alk	17639.79	557714	513049.09	430259.41
n-Hexadecane	C16alk	20649.75	734218.37	604105.68	552136.13
n-Heptadeane	C17alk	39436.57	957712.12	756239.11	734694.32
Pristane	Pristane	179030.58	1062569.99	1011699.98	941078.01
n-Octadecane	C18alk	18285.92	950172.49	715830.61	682853.69
Phytane	Phytane	130251.24	770151.81	671459.11	608225.69
Nonadecane	C19alk	20842.6	804240.37	555227.18	570488.82
n-Eiosane	C20alk	42970.64	991288.31	768994.99	734401.38
n-Heneicosane	C21alk	41379.91	917654	709135.61	692885.32
n-Docosane	C22alk	34859.66	697642.37	546757.62	394905.32
n-Tricosane	C23alk	30646.01	652961.31	512692.3	368755.41
n-Tetracosane	C24alk	53774.23	731496.5	587297.99	414241.82
n-Pentacosane	C25alk	57248.06	693386.31	567897.99	397817.69
n-Hexacosane	C26alk	76740.74	672339.5	551170.37	364412.91
n-Heptacosane	C27alk	88467.81	521234.31	426626.09	7359.9
n-Octacosane	C28alk	92329.51	376487.69	338775.99	279440.41
n-Nonacosane	C29alk	88025.76	346493.31	304533.4	280439.91
n-Triacontane	C30alk	88677.05	304725.59	268997	239246.8
n-Dotriacontane	C32alk	61988.65	209966.59	178576	166991.7
n-Tetratriacontane	C34alk	66300.84	268812.19	212083.79	199852.6
Unresolved Complex Mix	UCM	30890769.79	125199999.32	108099998.23	94320000.82